

---

**Article:**
Peitzsch, Claudia, Cojoc, Monica, Hein, Linda et al. (17 more authors) (2016) An epigenetic reprogramming strategy to re-sensitize radioresistant prostate cancer cells. Cancer research. pp. 2637-2651. ISSN 1538-7445

https://doi.org/10.1158/0008-5472.CAN-15-2116

---

# An epigenetic reprogramming strategy to re-sensitize radioresistant prostate cancer cells.

Claudia Peitzsch[1], Monica Cojoc[1*], Linda Hein[1*], Ina Kurth[1], Katrin Mäbert[1], Franziska Trautmann[1], Barbara Klink[2, 3], Evelin Schröck[2, 3], Manfred P. Wirth[4], Mechthild Krause[1, 3, 5, 6], Eduard A. Stakhovsky[7], Gennady D. Telegeev[8], Vladimir Novotny[4], Marieta Toma[9], Michael Muders[9], Gustavo B. Baretton[9], Fiona M. Frame[10], Norman J. Maitland[10], Michael Baumann[1, 3, 4, 6], Anna Dubrovska[1, 3, 6§]

[1] - OncoRay-National Center for Radiation Research in Oncology, Faculty of Medicine and University Hospital Carl Gustav Carus, Technische Universität Dresden and Helmholtz-Zentrum Dresden-Rossendorf, Fetscherstrasse 74, 01307 Dresden, Germany;

[2] - Institute of Clinical Genetics, Faculty of Medicine and University Hospital Carl Gustav Carus, Technische Universität Dresden, Fetscherstrasse 74, 01307 Dresden, Germany;

[3] - German Cancer Consortium (DKTK) Dresden and German Cancer Research Center (DKFZ) Heidelberg;

[4] - Department of Urology, Faculty of Medicine and University Hospital Carl Gustav Carus, Technische Universität Dresden, Fetscherstrasse 74, 01307 Dresden, Germany;

[5] - Department of Radiation Oncology, Faculty of Medicine and University Hospital Carl Gustav Carus, Technische Universität Dresden, Fetscherstrasse 74, 01307 Dresden, Germany;

[6] - Helmholtz-Zentrum Dresden-Rossendorf, Institute of Radiation Oncology, Bautzner Landstrasse 400, 01328 Dresden, Germany;

[7] - National Cancer Institute, Lomonosova Str, 33/43, Kyiv 03022, Ukraine;

[8] - Institute of Molecular Biology and Genetics NAS of Ukraine, Zabolotnogo Str, 150 Kyiv 03143, Ukraine

[9] - Department of Pathology, Faculty of Medicine and University Hospital Carl Gustav Carus, Technische Universität Dresden, Fetscherstrasse 74, 01307 Dresden, Germany;

[10] - YCR Cancer Research Unit, Department of Biology, University of York, Heslington, YO10 5DD, North Yorkshire, UK

* - These authors contributed equally to this work

§- To whom correspondence should be addressed:

OncoRay-National Center for Radiation Research in Oncology, Medical Faculty and University Hospital Carl Gustav Carus, Technische Universität Dresden, Fetscherstr.74/PF41 01307 Dresden, Germany

E-mail: Anna.Dubrovska@OncoRay.de

**COI declaration:** Authors declare that they have no conflict of interest.

**Running title:** Targeting of the epigenetic reprogramming for radiosensitization

**Abstract**

Radiation therapy is a mainstay of curative prostate cancer treatment, but risks of recurrence after treatment remain significant in locally advanced disease. Given that tumor relapse can be attributed to a population of cancer stem cells (CSC) that survive radiation therapy, analysis of this cell population might illuminate tactics to personalize treatment. However, this direction remains challenging given the plastic nature of prostate cancers following treatment. We show here that irradiating prostate cancer cells stimulates a durable upregulation of stem cell markers that epigenetically reprogram these cells. In both tumorigenic and radioresistant cell populations, a phenotypic switch occurred during a course of radiotherapy that was associated with stable genetic and epigenetic changes. Specifically, we found that irradiation triggered histone H3 methylation at the promoter of the CSC marker aldehyde dehydrogenase 1A1 (*ALDH1A1*), stimulating its gene transcription. Inhibiting this methylation event triggered apoptosis, promoted radiosensitization and hindered tumorigenicity of radioresistant prostate cancer cells. Overall, our results suggest that epigenetic therapies may restore the cytotoxic effects of irradiation in radioresistant CSC populations.

**Keywords:** Prostate cancer stem cells, radiotherapy, radiosensitivity, reprogramming, histone 3 methylation, ALDH1

## Introduction

Prostate cancer is the most common cancer among men and the third leading cause of cancer-related deaths in men worldwide[1]. A significant proportion of prostate cancer patients are diagnosed with potentially curable localized tumor which can be treated with surgery and radiotherapy alone or in combination with androgen ablation. Tumor radioresistance can be a limiting factor of the efficacy of radiotherapy for some patients with a high-risk prostate cancer[2, 3]. Depending on the stage of disease, up to 45% of prostate cancers can relapse after radiotherapy[4-6]. Tumor relapse after radiotherapy has been attributed to the population of cancer stem cells (CSCs) or tumor initiating cells[7-9]. The cancer stem cell hypothesis argues that cancer cells are hierarchically organized according to their tumorigenic potential, and tumors are initiated and maintained by the populations of CSCs[10]. Decades of radiobiological research have demonstrated that the frequency of tumor cells with CSC characteristics and their intrinsic radiosensitivity varies between tumors[7, 11, 12]. Radiobiological studies provided evidence for the importance of these cells for local tumor control and suggested that efficient tumor treatment by irradiation might require eradication of the entire CSC population. The role of CSCs in tumor development and recurrence has recently motivated investigations of CSC-specific biomarkers for the analysis of CSC populations in tumor pre-treatment biopsies for prediction of clinical outcome and selection of the optimal treatment strategy [13, 14]. It is also assumed that the combination of radiotherapy with agents which target or radiosensitize the CSC population might be beneficial for the treatment refinement[14]. However, compelling evidence suggests a high diversity of CSCs and plasticity of their features imposed by tumor treatment, which could challenge the development of CSC-related predictive biomarkers and CSC-targeted therapy. Furthermore, CSCs, which are selected or induced following chemo- or radiotherapy, are very difficult to detect before treatment, and might acquire treatment resistance resulting in tumor relapse[15].

In the present study we show that irradiation induces genetic and epigenetic alterations that affect prostate cancer cell tumorigenicity and radioresistance. The epigenetic changes driven by irradiation were mediated by histone methylation, which induced the expression of *ALDH1A1* gene regulating the maintenance of the prostate CSCs and their radioresistance. Targeting of the histone 3 methylation with DZNep, an inhibitor of lysine methyltransferase enhancer of zeste homologue 2 (EZH2), led to the downregulation of *ALDH1A1* expression and tumor cell radiosensitization.

Furthermore, irradiation causes long-term alterations in the expression of stem cell markers and induces tumor cell reprogramming. To our knowledge this is the first study demonstrating that radioresistant cell populations within prostate cancer cells undergo a phenotypic switch during the course of irradiation. We found that in contrast to non-irradiated cells, ALDH activity is not indicative of a radioresistant cell subset in the cells surviving the course of fractionated irradiation. Moreover, our study demonstrates that radioresistant prostate cancer cells are more sensitive to the DZNep treatment, which induces apoptosis and abrogates tumorigenicity in combination with X-ray irradiation.

Our findings suggest that radioresistant properties of cancer cells are dynamic in nature and that a combination of radiotherapy with drugs which prevent tumor cell reprogramming may be beneficial for eradication of tumor initiating and radioresistant cell populations. Future research must extend this work by using additional experiments on primary cultures and biopsies, and by combination of DZNep treatment with radiation therapy in xenograft mouse models of human prostate cancer.

## Materials and methods

### Cell lines and culture condition

Prostate cancer cell lines DU145, PC3 and LNCaP were purchased from the American Type Culture Collection (ATCC, Manassas, VA) and cultured according to the manufacturers recommendations in a humidified 37°C incubator supplemented with 5% $CO_2$. DU145 and PC3 cell lines were maintained in Dulbecco's Modified Eagle's Medium (DMEM) (Sigma-Aldrich) and LNCaP cells in RPMI-1640 medium (Sigma-Aldrich) containing 10% fetal bovine serum (FBS, PAA Laboratories) and 1mM L-glutamine (Sigma-Aldrich). Radioresistant (RR) cell lines were established as described earlier[16]. The RR cells were kept in culture up to 6 months after the last irradiation and their radioresistance were confirmed by radiobiological cell survival assays. The corresponding age-matched non-irradiated parental cells were used as controls for RR cell lines. Human papillomavirus 18 (HPV 18) immortalized, non-tumorigenic RWPE1 cells were purchased from the American Type Culture Collection (ATCC, Manassas, VA) and maintained in the complete keratinocyte growth medium, K-SFM (Invitrogen) supplemented with 50μg/ml of bovine pituitary extract (BPE) and 5 ng/ml of epidermal growth factor (EGF). All cell lines were genotyped using microsatellite polymorphism analysis and tested for mycoplasma directly prior to experimentation.

Human prostate tumor primary cells were obtained from Prof. Norman J. Maitland laboratory at the YCR Cancer Research Unit, University of York, UK. Primary cell culture 311/13 was established from 67 years old prostate cancer patient with Gleason Score 3+4 = 7, pT2c, preoperative PSA 8.7 ng/ml. Primary cell culture 312/13 was established from 66 years old prostate cancer patient with Gleason Score 3+4 = 7, pT2c, preoperative PSA 6.6 ng/ml. Epithelial cell cultures were prepared and characterized as described previously, and maintained in stem cell medium containing keratinocyte growth medium supplemented with 5 ng/ml of epidermal growth factor (EGF), bovine pituitary extract (BPE) (Invitrogen, DE),

2 ng/ml leukemia inhibitory factor (LIF) (Peprotech, DE) 2 ng/ml stem cell factor (SCF) (Peprotech, DE), 100 ng/ml cholera toxin (Sigma-Aldrich Company Ltd, DE) and 1 ng/ml granulocyte macrophage colony-stimulating factor (GM-CSF) (Miltenyi, DE)[17]. Cells were cultured in the presence of irradiated (60 Gy) STO (mouse embryonic fibroblast) cells. After expansion, the primary epithelial cells were plated at density of $8x10^4$ cells/ml in collagen I coated chamber slides (Corning, DE) without feeder cells. Cell were pretreated with DMSO (control cells) or DZNep at concentration of 1μM for 24 h, irradiated with 4 Gy or left non-irradiated and fixed with 4% formaldehyde 24 h after irradiation. Primary prostate cells were used for the experiments at the early passages (up to 6 passages for the cells from patient 312/13 and up to 5 passages for the cells from patient 311/13).

**Human tissue samples**

Clinical material was collected at Department of Urology, University Hospital Carl Gustav Carus, Technische Universität Dresden and Kyiv National Cancer Institute with informed consent and approval from the local ethics committee (Institutional review board of the Faculty of Medicine, Technische Universität Dresden, EK49022015 and Ethics Committee of Kyiv National Cancer Institute, protocol no. 44, correspondingly). The tumor specimen PT1 was taken from a lymph node of a 69 years old patient (pT3bpN1L1V0R0G3a, Gleason Score 4+3=7, preoperative PSA level 6.58 ng/ml) with newly diagnosed prostate cancer, who underwent primary surgery (bilateral lymphadenectomy and prostate-vesiculectomy). The tumor specimen PT2 is a radical prostatectomy tissue taken from a 64 years old patient (pT2c N0 M0, Gleason Score 3+4=7, preoperative PSA level 19.8 ng/ml). The tumor specimen PT3 is a radical prostatectomy tissue taken from 48 year old patient (pT3apN0L0V0Pn1, Gleason Score 4+3=7, preoperative PSA level 10.7 ng/ml).

**Human tumor tissue ex vivo culture**

Tumor tissue samples were cut into small pieces of approximately 3 mm x 3 mm and transferred to 12 well ultra-low attachment plates (Corning) in MEBM medium (Lonza,

Germany) supplemented with 4 µg/ml insulin (Sigma-Aldrich), B27 (Invitrogen), 20 ng/mL epidermal growth factor (EGF) (Peprotech), 20 ng/ml basic fibroblast growth factor (FGF) (Peprotech). The tissues were treated with 2µM of DZNep for 24h, consequently irradiated with 4 Gy of X-ray and fixed 24 h after irradiation. Tissue fragments incubated under the same conditions but treated with DMSO and sham-irradiation were used a control. The presence of tumor cells in the tissue pieces was analyzed by hematoxylin and eosin staining, by fluorescent immunostaining with PSMA and CK5/14 antibody and was confirmed by a pathologist.

**Animals and in vivo tumorigenicity assay**

The animal facilities and the experiments were approved according to the institutional guidelines and the German animal welfare regulations (protocol number TW_2014_30). The experiments were performed using 8 to 12-weeks-old male NMRI (nu/nu) mice that were bred in-house (Experimental Centre, Faculty of Medicine, Technische Universität Dresden). To immunosuppress the nude mice further, the mice underwent total body irradiation 1-3 days before tumor transplantation with 4 Gy (200 kV X-rays, 0.5 mm Cu filter, 1 Gy/min). Mice were examined once a week and the relative tumor volumes ($mm^3$) based on caliper measurements were calculated as (length × width × height)/2. At a tumor volume of 100 $mm^3$ mice were scored as tumor bearing to calculate tumor uptake. Kaplan-Meier plots were analyzed using the log rank test (Graph Prism 5). Analysis of the tumor initiating cell numbers was performed using the web-based ELDA (Extreme Limiting Dilution Analysis) statistical software at http://bioinf.wehi.edu.au/software/elda/index.html, which uses the frequency of tumor positive and negative animals at each transplant dose to determine the number of tumor initiating cells within the injected cell populations[65]

**Microarray analysis of the prostate cancer cell lines**

Gene expression profiling of the DU145, DU145-RR, $ALDH^+$ DU145, $ALDH^-$ DU145, $ALDH^+$ DU145-RR, $ALDH^-$ DU145-RR cells was performed using SurePrint G3

Human Gene Expression 8x60K v2 Microarray Kit (Design ID 039494, Agilent Technologies) according to manufacturer's recommendations. Total RNA was isolated from cell pellets using the RNeasy kit (Qiagen, Valencia, CA, USA). Sample preparation for analysis was carried out according to the protocol detailed by Agilent Technologies (Santa Clara, CA, USA). Briefly, first and second cDNA strands were synthesized; double stranded cDNA was in vitro transcribed using the Low Input Quick Amp Labeling Kit; and the resulting cRNA was purified and hybridized to oligonucleotide arrays representing about 60,000 features, including 27,958 Entrez Gene RNAs and 7,419 lincRNAs. Arrays were processed using standard Agilent protocols. Probe values from image files were obtained using Agilent Feature Extraction Software. The dataset was normalized using GeneSpring software, and the list of differentially regulated genes with fold change > 2 and p-value < 0.05 was further analyzed using the web-based Panther Pathway Analysis tool (http://www.pantherdb.org/tools/index.jsp). Data deposition: all data is MIAME compliant and that the raw data has been deposited in the Gene Expression Omnibus (GEO) database, accession no GSE53902, http://www.ncbi.nlm.nih.gov/geo/query/acc.cgi?acc=GSE53902.

**Immunofluorescence microscopy**

Cells were plated in a 96 well black clear bottom plates (Greiner Bio-One) at a density of 1000 cells/well in medium containing 10% serum. After 18 hours the cells were fixed for 30 min with 3.7% formaldehyde at room temperature and permeabilized with 0.125% Triton X-100 for 10 min followed by washing with PBS, and blocked by incubation with 10% BSA in PBS. The cells were then incubated for 12 h at 4$^{o}$C with primary antibody against phospho-histone H2AX (S139) (Millipore, Hamburg, Germany), β-catenin (#D10A8, Cell Signaling Technology), ALDH1A1 (clone H-4, Santa Cruz), PARP cleaved (Asp214) (#5625, Cell Signaling Technology) or ALDH1A3 (HPA046271, Sigma-Aldrich) diluted in 3% BSA in PBS as 1/100 and washed ten times with PBS. Cells were then incubated for 0.5 h with a secondary antibody conjugated with Alexa Fluor 488 or 555 (Invitrogen) diluted 1/500 in 3%

BSA in PBS. After appropriate washes with PBS, the cells were stained with DAPI and examined by fluorescent microscopy. For quantification, 200 to 1000 cells per condition in at least three randomly selected fields were counted. Nuclear intensity of γH2A.X and cleaved PARP signal was evaluated using ImageJ software.

**Clonogenic cell survival assay**

Cells were plated at a density of 500-2000 cells/well depending on the cell line in 6-well plates and irradiated with doses of 2, 4, 6 and 8 Gy of 200 kV X-rays (Yxlon Y.TU 320; dose rate 1.3Gy/min at 20 mA) filtered with 0.5 mm Cu. The absorbed dose was measured using a Duplex dosimeter (PTW). After 10 days, the colonies were fixed with 10% formaldehyde (VWR) and stained with 0.05% crystal violet (Sigma-Aldrich). Colonies containing > 50 cells were counted using a stereo microscope (Zeiss). The plating efficiency (PE) was determined as the ratio between the generated colonies and the number of cells plated. The surviving fraction (SF) was calculated as the PE from the irradiated cells divided by the PE from the non-irradiated control. For 3D colony formation analysis, a cell suspension (500 cells $ml^{-1}$) in 0.2% low-melting SeaPlaque CTG agarose (Cambrex Bio Science Rockland, Inc.) with MEBM medium (Lonza, Germany) supplemented with 4 µg/ml insulin (Sigma-Aldrich), B27 (Invitrogen), 20 ng/mL epidermal growth factor (EGF) (Peprotech), 20 ng/ml basic fibroblast growth factor (FGF) (Peprotech) was overlaid into 24-well low attachment plates (Corning). All samples were plated in triplicates. The plates were incubated at 37 °C in a humidified incubator for 14 days.

**Sphere formation assay**

To evaluate the self-renewal potential, cells were grown as non-adherent multicellular cell aggregates (spheres). Cells were plated at a density of 1000 cells/2 ml/well in 6 well ultra-low attachment plates (Corning) in MEBM medium (Lonza, Germany) supplemented with 4 µg/ml insulin (Sigma-Aldrich), B27 (Invitrogen), 20 ng/mL epidermal growth factor (EGF) (Peprotech), 20 ng/ml basic fibroblast growth factor (FGF) (Peprotech). Media containing

supplements were exchanged once a week and spheres with a size > 100 μm were assayed after 14 days using Axiovert 25 microscope (Zeiss) or were automatically scanned using the Celigo S Imaging Cell Cytometer (Brooks). Sphere number and size were calculated using ImageJ software.

**Cell proliferation and cytotoxic activity**

Cell proliferation and cytotoxicity was analyzed using the MTT assay (Sigma-Aldrich). $3x10^3$ cells/well were seeded into 96-well plates and quantified after 1-4 days at 560 nm absorbance, with reference at a wavelength of 690 nm using a microplate reader (Tecan).

**Transwell migration assay**

Prostate cancer cells were starved for 24 h under serum-free conditions. 10.000 cells were plated on top of the membrane with 8 μm pore size (Boyden chamber, BD Bioscience) in a 24-well plate. After 24 h membranes were fixed with 10% para-formaldehyde and stained with 0.04% crystal violet. Absolute migration was evaluated by counting migrating cells on the membrane using Axiovert25 microscope (Zeiss, Germany).

**Western blot analysis and chemical inhibitors**

XAV939, BIX01295 and DZNep inhibitors were purchased from Biomol GmbH. DMSO was used at concentration ≤1% v/v DMSO as a drug solvent, and corresponding concentrations of DMSO were used as controls in all the experiments which included cell treatment. Cells were lysed in RIPA buffer (Santa Cruz) and protein concentrations were determined using the bicinchoninic acid assay (BCA) according to manufacturer's recommendations (Pierce). All antibodies were used at concentrations recommended by the supplier followed by the incubation with a 1:5000 dilution of appropriate HRP-conjugated secondary antibody (Santa Cruz Biotechnology). The signal was visualized using the enhanced chemiluminescence detection reagent (GE Healthcare). Semi-quantitative analysis of protein expression relative to the loading control β-actin or GAPDH was performed with ImageJ software.

**Flow cytometry analysis**

For single cell analysis and multi-color staining, cells were dissociated with Accutase (PAA) and stained at 4°C in PBS buffer with 1mM Ethylenediaminetetraacetic acid (EDTA) and 5% FBS according to the manufactures protocol. Aldehyde dehydrogenase activity was analyzed using Aldefluor assay (Stem Cell Technologies) according to manufacturer's protocol. Samples were analyzed with the BD LSRII flow cytometer (Beckton Dickinson). A minimum of 100,000 viable cell events were collected per sample. Data were analyzed using FlowJo software (version 7.6.2) and gates were set according to the individual isotype controls. To purify $ALDH^+$ cell population, cells were stained using the Aldefluor assay (Stem Cell Technologies). Cells incubated with the specific ALDH inhibitor diethylaminobenzaldehyde (DEAB) served as negative control. Dead cells were excluded by 1µg/ml DAPI staining and doublets were excluded using the FSC-W&H and SSC-W&H function of the BD FACSDiva 6.0 software. $ALDH^+$ and $ALDH^-$ populations were sorted on a BD FACS Aria III (Beckton Dickinson) using 100 µm nozzle with an average purity of > 90%.

**Chromatin immunoprecipitation assay**

Chromatin immunoprecipitation assays were performed using the ChIP Assay Kit (17-295, Millipore) according to the manufacturer's instructions. DNA shearing was performed using Covaris S2 ultrasonicator under the following conditions: intensity 4, duty cycle 10%, cycles per burst 200, treatment time 55 sec. The following antibodies were used to immunoprecipitate DNA: anti-H3 (D2B12, Cell Signaling Technology), anti-H3K36me3 (D5A7, Cell Signaling Technology) and normal rabbit IgG (Cell Signaling Technology).

**Luciferase reporter assay**

ALDH1A1-promoter luciferase reporter was purchased from Switchgear genomics. M50 Super 8x TOPFlash and M51 Super 8x FOPFlash (TOPFlash mutant) were a gift from Randall Moon (Addgene plasmid # 12456 and # 12457) (1). Transient transfection of plasmid

DNA in DU145 and LNCaP cells was performed using Lipofectamine 2000 (Life Technologies GmbH) according to the manufacturer's instruction. Luciferase activity was normalized to FOP-Flash reporter. Luciferase assay was conducted using LightSwitch Assay (Switchgear genomics) or Bright-Glo™ luciferase assay system (Promega).

**Histology**

Human tumor specimens were fixed by immersion in 4% paraformaldehyde, cryoprotected in 30% sucrose and embedded in TissueTek O.C.T compound (Sakura Finetek). The 10 µm thick tissue sections (Microm HM 560, Cryo-Star Cryostat) were collected on Superfrost plus slides (Thermo Fisher Scientific). Slides were blocked for 1 h in PBS buffer containing 10% of horse serum and 0,4% TritonX100 and then incubated overnight at 4°C with the primary antibodies against EpCAM (sc-21792, Santa Cruz), γH2A.X (05-656, Millipore) and PARP cleaved (Asp214) (#5625, Cell Signaling Technology). Staining with antibody against CK5/14 (#C1857C01, DCS Innovative Diagnostik-Systeme, clone XM26/SFI-3) was used to distinguish benign prostate glands (CK5/14 positive) from cancer glands (CK5/CK14 negative). Bound antibodies were detected with appropriate secondary antibodies conjugated with AlexaFluor 488 or 555 (Molecular Probes) at room temperature for 1 h. Slides were analyzed using the Meta Confocal Microscope (LSM510, Zeiss). Images were analyzed using ImageJ software. For quantification, two independently treated tissue pieces validated for the presence of tumor cells were analyzed for each condition.

**Determination of GSH and ROS levels**

To analyze GSH level, cells were stained with 40µM monochlorobimane (mBCI; Life Technologies) for 30 min at 37°C, washed with PBS at the end of culture and analyzed by Celigo cytometer. To measure the level of reactive oxygen species (ROS) cells were incubated with 5µM 5-(and-6)-carboxy-2',7'-dichlorodihydrofluorescein diacetate acetyl ester (CMH2DCFDA, Invitrogen Molecular Probes) for 15 min at 37°C. Samples were analyzed with the BD LSRII flow cytometer (Beckton Dickinson). A minimum of 100,000 viable cell

events were collected per sample. Data were analyzed using FlowJo software (version 7.6.2) and gates were set according to the individual controls.

**Array Comparative Genome Hybridization (array-CGH)**

Array-CGH was performed on Agilent's SurePrint G3 Human CGH+SNP Microarray Kit 2x400K (Design ID 028081, Agilent, Santa Clara, CA, USA) according to the manufacturer's instructions with the exception that the labeling of reference and test DNA was reversed. Arrays were scanned using an Agilent microarray scanner. Agilent's CytoGenomics Editions 2.7 and 2.9 were used for extraction and processing of Raw data (using the integrated Feature Extraction software) and to determine deleted and amplified regions based on the draft of the reference human genome (GRCh37/hg19) using the Default Analysis Method - CGH v2. All results were additionally checked by eye and were evaluated by a board-certified medical geneticist (Barbara Klink). CNVs that were commonly found in the Database of Genomic Variants (http://dgv.tcag.ca/) and therefore can be considered as polymorphisms that are most likely germline were excluded from further analysis.

**Statistical analysis**

The results of colony formation assays, microscopy image analysis, gene reporter assay, ChIP assay, cell migration, flow cytometry analysis, cell proliferation assays, gene expression and siRNA-mediated gene silencing were analyzed by paired t-test. Tumor uptake rate was calculated using log-rank (Mantel-Cox) test. Multiple comparison analysis for the data depicted on Figures 2D, S9B and S9C was performed using one-way ANOVA analysis by GraphPad Prism software. The differences between cell survival curves depicted on Figures 3A, 3F, 4C and S7C were analyzed using the statistical package for the social sciences (SPSS) v23 software as described by Franken et al[18] by fitting the data into the linear-quadratic formula $S(D)/S(0)=\exp(\alpha D+\beta D^2)$ using stratified linear regression. A p value of $< 0.05$ was regarded as statistically significant. $IC_{50}$ values were calculated by fitting the curves with nonlinear regression using GraphPad Prism software.

## Results

### *Irradiation causes long-term alterations in the expression of stem cell markers*

In our previous studies we have shown that radioresistant sublines obtained by multiple irradiation of prostate cancer cell lines with 4 Gy of X-ray *in vitro* are characterized by an increased expression of stem cell markers and enhanced tumorigenicity in mice[16]. Here, we analyzed the time-dependent effect of irradiation on the expression of different CSC markers and activation of pro-survival pathways in parental (P) and radioresistant (RR) DU145 and LNCaP cells (Figure S1A). Irradiation of DU145 and LNCaP cells with a single X-ray dose of 4 Gy led to long-term and time-dependent changes in the cell phenotype, such as enhanced ALDH activity, increased expression of stem cell markers including OCT4, NANOG, BMI1, ABCG2, activation of PI3K/AKT signaling pathway and gain of epithelial-mesenchymal transition (EMT) signatures such as upregulation of the β-catenin and vimentin expression (Figure 1AB, Figure S1BC). The expression level of these stem cell markers and EMT signatures continuously increased during three to four weeks after irradiation and was correlated with an increase in clonogenic potential of DU145 and DU145-RR cells (Figure 1C).

Fractionated irradiation with more than 56Gy (14x4Gy) of X-rays resulted in the establishment of cell sublines with a stable radioresistant phenotype which have upregulated CSC marker expression, increased migratory potential and high tumorigenicity *in vivo*[16] (Figure S1D). We and others have shown that prostate cancer cells with a high ALDH activity ($ALDH^+$) have functional characteristics of tumor initiating cells[16, 19]. We found that irradiation might cause $ALDH^+$ cell enrichment in both, $ALDH^+$ and $ALDH^-$ cell populations isolated by fluorescence-activated cell sorting (FACS) from DU145 prostate cancer cells and cultured in serum containing medium for two weeks (Figure 1D). Notably, the $ALDH^+$ cell population did not show an increased proliferation in response to irradiation, as compared to

ALDH$^-$ cells (Figure S1E). These results suggest that irradiation can not only select but also induces a prostate tumor cell population with CSC features. Taken together, these findings have shown that irradiation might influence cell clonogenicity and radioresistance, and has a long term effect on the expression of stem cells markers and cell phenotype.

***Irradiation induces epigenetic and genetic alterations in prostate cancer cells***

Our previous studies demonstrated that regrowth of DU145 xenograft tumors after chemotherapy can be attributed to certain genetic aberrations which leads to an increase in tumor initiating cells[20]. Microsatellite polymorphism analysis revealed genetic alterations in DU145-RR cells as compared to the parental DU145 cells suggesting that X-ray treatment might induce genomic instability in prostate cancer cells[21] (Figure S2A).

To identify genomic aberrations in the irradiated prostate cancer cells more comprehensively, we analyzed DNA from DU145 and DU145-RR cells using comparative genome hybridization (CGH) microarray. CGH array revealed a high number of various copy number variations (CNVs) in parental DU145 cells, including partial chromosome deletions and duplications (e.g. partial gains and losses on chromosome 4). There were also marked differences between the paternal and radioresistant cells (Figure S2BC). Noteworthy, comparative analysis of the gene expression profiling and CGH data revealed that 53,5% (711 out of 1328) differentially regulated genes ( $\geq$ 2 fold, $p < 0.05$) for the parental and radioresistant DU145 cells did not mapped to within the deleted or amplified chromosomal regions. This suggests that expression of these genes is mediated by genetic alterations in other genes or by epigenetic mechanisms (Table S1). Gene expression profiling of the parental and radioresistant prostate cancer cells and FACS-isolated ALDH$^+$ and ALDH$^-$ cell populations revealed changes in the expression level of a number of genes involved in the epigenetic regulation of protein expression through DNA and histone modification (Figure

2A). To determine the biological processes that are activated in radioresistant cells, we performed a gene set enrichment analysis (GSEA) based on the 3553 features that were significantly upregulated by ≥1.5 fold ($p < 0.05$) in DU145-RR as compared to parental DU145 cells. Analysis of the existing gene sets deposited in the MSigDB (molecular signature database) revealed that DU145-RR up-regulated genes have a strong association with epithelial mesenchymal transition, stemness, activation of WNT and other pro-survival pathways and histone modifications (Figure 2B, Table S2).

We next investigated whether irradiation induces global chromatin modifications. Methylation of lysine residues K4 and K36 in histone H3 correlates with transcriptional activation, whereas trimethylation of histone H3 on lysine 27 enforces gene silencing[21]. We found that irradiation induced long-term changes in H3K4, H3K36 and H3K27 tri-methylation in prostate cancer cells, which can be observed at least 6 weeks after treatment (Figure 2C, Figure S3A). In accordance with this observation, western blot analysis revealed long-term and time-dependent changes in the expression of the histone methyltransferases involved in H3 methylation on residues K27 (EZH2) or K36 (SETD2) (Figure S3AB). In addition, Ingenuity Pathway Analysis (IPA) revealed histone methyltransferase EZH2 as one of the most significantly upregulated transcriptional regulators in DU145-RR cells as compared to parental cells (p value $< 10^{-8}$) (Figure S3C). Interestingly, H3K4 and H3K36 tri-methylation increased during TGFβ-induced EMT and cell reprogramming[21] and was significantly upregulated in the highly migratory DU145-RR and LNCaP-RR cells as compared to their non-irradiated parental counterparts, as well as in parental DU145 cells after irradiation (Figure 2D, Figure S3D). In contrast, radioresistant cells showed no significant change in H3K4 and H3K36 methylation in response to irradiation (Figure 2D). In line with this observation, we found that DU145-RR and LNCaP-RR cells display an increased basal expression of EMT and stem cell markers which was altered after irradiation to a lesser extent than in parental cell lines (Figure 1AB, Figure S4A). Moreover, irradiation

induced an $ALDH^+$ cell population to a lesser degree in both DU145-RR $ALDH^+$ and DU145-RR $ALDH^-$ cell populations, as compared to the $ALDH^+$ and ALDH- cells isolated from the parental cells (Figure S4B).

To determine whether histone H3 methylation can regulate *ALDH1A1* gene transcription after X-ray irradiation, a chromatin immunoprecipitation assay (ChIP) was performed. The cross-linked DNA-protein complexes from X-ray irradiated or non-irradiated parental and DU145-RR cells were immunoprecipitated either with anti-H3K36me3 or with anti-H3 and control IgG antibodies. PCR amplification was performed using primers flanking two regions of the ALDH1A1 promoter containing binding sites for β-catenin/TCF transcription factor and named ALDH1A1 i and ALDH1A1 ii with sizes of 508 b.p. and 518 b.p. correspondingly[16, 22] (Figure 2E). The results of the ChIP analysis showed that the H3K36 methylation mark at *ALDH1A1* promoter increased after irradiation with 4Gy of X-ray (Figure 2E). To perform a direct analysis of the transcriptional regulation of *ALDH1A1*, we used a reporter system where luciferase gene expression is regulated by the endogenous *ALDH1A1* gene promoter. The results of the luciferase reporter assay confirmed that *ALDH1A1* transcription is highly activated in the RR prostate cancer cell lines and irradiation of parental cells led to a significant increase of *ALDH1A1* transcription as well as to upregulation of β-catenin/TCF reporter gene expression (Figure 2F, Figure S5A). These results suggest an epigenetic regulation of *ALDH1A1* transcription by irradiation, which is mediated by histone H3 methylation and is consistent with flow cytometry data for the ALDH enzymatic activation in response to irradiation (Figure 1B). Taken together, these findings suggest that genetic alterations and changes in the histone methylation which have occurred during treatment contribute to the emergence of cell radioresistance and stem cell reprogramming.

***Characterization of the properties of ALDH$^+$ and ALDH$^-$ cell populations in radioresistant prostate cancer cells***

Our previous study demonstrated that ALDH activity is indicative of prostate tumor initiating cells with increased radioresistance[16]. Chemical inhibition of ALDH activity as well as knockdown of ALDH1A1 mediated by siRNA resulted in a significant decrease in prostate cancer cell ALDH activity, spherogenicity and radioresistance (Figure S5BCD)[16] suggesting that ALDH activity and cell radioresistance not only correlate but are causally linked.

Taking into account the genetic, phenotypical and functional differences between the parental and radioresistant prostate cancer cell lines, we hypothesized that irradiation can induce plasticity of the tumor stem cell phenotype. To test this assumption, we performed a comparative analysis of the spherogenic, tumorigenic and radioresistance properties of ALDH$^+$ and ALDH$^-$ cell subsets isolated from the parental and DU145-RR cell line. Similarly to the DU145 ALDH$^+$ cells, DU145-RR ALDH$^+$ cells showed an increase in sphere forming potential over DU145-RR ALDH$^-$ cells (Figure S5E). To analyze the tumorigenic potential of DU145-RR ALDH$^+$ and DU145-RR ALDH$^-$ populations, the FACS purified cells were injected s.c. into athymic immunodeficient NMRI nu/nu mice at varying cell numbers (100, 1000 and 3000 cells). The DU145-RR ALDH$^+$ population showed a significantly higher frequency of tumor initiating cells than the DU145-RR ALDH$^-$ cell population (1/961, at 95% confidence interval: 1/2061 to 1/448 cells vs. 1/4637, at 95% confidence interval: 1/10558 to 1/2037 cells, respectively; p-value < 0.01) (Figure S5F). When the radioresistance of the two populations was compared DU145-RR ALDH$^+$ and DU145-RR ALDH$^-$ cells showed similar responses, unlike the ALDH$^+$ and ALDH$^-$ cell populations isolated from the parental DU145 cell line. No significant differences in the radiobiological response of DU145-RR ALDH$^+$ and DU145-RR ALDH$^-$ cells were observed in either the 2D or the 3D survival assays (Figure 3A, Figure S5G).

The phosphorylation of histone H2A.X by ATM or ATR protein kinases on the sites of DNA damage is a marker of DNA double strand break (DSB) response. Residual nuclear foci of the phosphorylated H2A.X (γ-H2A.X), measured 24h after irradiation, are associated with DNA lesions which cannot be repaired and can lead to cell death[23, 24]. We have recently reported that $ALDH^+$ cell population among the non-irradiated prostate cancer cells has a lower level of DNA double-strand breaks and more efficient DNA repair after irradiation as compared to the $ALDH^-$ cells. We found that, in contrast to the parental DU145 cells, the number of residual γ-H2A.X foci 24h after irradiation was not increased in DU145-RR $ALDH^+$ cells compared to DU145-RR $ALDH^-$ cells (Figure S5H). Various ALDH isoforms contribute to the high ALDH activity in prostate cancer cells including ALDH1A1 and ALDH1A3, which show abundant expression in prostate cancer tissues[25]. Both of these isoforms are expressed at high levels in the radioresistant prostate cancer cell lines, and in the $ALDH^+$ cell populations[16] (S6ABC). Microscopy analysis of the residual γ-H2A.X foci in the ALDH1A3 positive DU145 and DU145-RR cells confirmed that, in contrast to the parental cells, ALDH1A3 expression in DU145-RR cells is not indicative of more efficient DNA DSB repair (Figure 3B). Taken together, this data suggest that, in contrast to the parental prostate cancer cells, ALDH activity is not a marker of more radioresistant cell population in cells with acquired radioresistance. These findings suggest that radioresistant prostate cancer cell populations can change their phenotype during the course of irradiation.

***Comparative gene expression profiles of $ALDH^+$ and $ALDH^-$ cell populations in parental and radioresistant prostate cancer cells***

To better understand the biological mechanisms which may underlie the lack of difference in radiosensitivity between $ALDH^+$ and $ALDH^-$ cell populations in cells with acquired radioresistance, we employed comparative gene expression profiling of $ALDH^+$ and $ALDH^-$ cells isolated from the parental DU145 cell line and from its radioresistant derivative

DU145-RR cell line. Whereas the differences between DU145 ALDH$^+$ and DU145 ALDH$^-$ cell populations are largely based on the deregulation of the WNT and cadherin signaling pathway, the distinct characteristics of the DU145-RR ALDH$^+$ and DU145-RR ALDH$^-$ cells depend on the differential regulation of DNA replication, which might be reflective of a high rate of DU145-RR ALDH$^+$ cell proliferation (Figure 3C, Figure S6D). Moreover, as indicated by the number of commonly regulated genes, the set of genes that is differentially expressed between DU145 ALDH$^+$ and DU145 ALDH$^-$ cells is more similar to the gene set which is differentially regulated between parental DU145 and DU145-RR cells, as compared to the genes which are differently expressed between DU145-RR ALDH$^+$ and DU145-RR ALDH$^-$ cells (Figure 3C).

Analysis of the genes that are involved in the WNT signaling pathway and differentially regulated between DU145 ALDH$^+$ and ALDH$^-$ population and between DU145 and DU145-RR cells revealed that expression of these genes does not differ between DU145-RR ALDH$^+$ and DU145-RR ALDH$^-$ cells except *WNT9A* (wingless-type MMTV integration site family, member 9A), which is significantly downregulated in DU145-RR ALDH$^+$ cells as compared to the DU145-RR ALDH$^-$ cell population (Table S3-S5). Consistent with this observation, hierarchical clustering analysis of the WNT signaling pathway genes that were significantly up- or downregulated by ≥1,5 fold ($p < 0.05$) in DU145-RR as compared to DU145 cells and in ALDH$^+$ versus ALDH$^-$ cells demonstrated that DU145-RR ALDH$^+$ and DU145-RR ALDH$^-$ cells cluster together. In contrast, DU145 ALDH$^+$ cells formed a cluster separated from DU145 ALDH- cells (Figure 3D).

Activation of the canonical WNT signaling pathway leads to the stabilization and nuclear accumulation of β-catenin, which interacts with T-cell factor/lymphoid enhancing factor-1 (TCF/LEF) proteins to regulate gene transcription. We found that ALDH$^+$ cells have a higher level of nuclear β-catenin, which is consistent with an activation of the WNT signaling pathway in this cell population[16]. In contrast to the parental DU145 cells, ALDH$^+$

and ALDH$^-$ cell populations isolated from DU145-RR cells both showed a high nuclear accumulation of β-catenin and no differences in its intracellular distribution (Figure 3E). WNT signaling, which is overrepresented in both radioresistant prostate cancer cells and ALDH$^+$ tumor initiating cell population is a potent inducer of EMT and cell migration[26]. We next analyzed the migratory properties of ALDH$^+$ and ALDH$^-$ cell populations isolated from the parental and radioresistant DU145 and LNCaP cell lines. The results of the Boyden-chamber based cell migration analysis demonstrated that in contrast to ALDH$^+$ and ALDH$^-$ cell subsets isolated from the radioresistant cell lines, ALDH$^+$ cells isolated from the parental cells lines have a higher migratory potential as compared to ALDH$^-$ cell population (Figure S6E). Inhibition of the WNT signaling by tankyrase inhibitor XAV939, which stimulates β-catenin degradation, led to the inhibition of cell clonogenicity and increases in cell radiosensitivity, with a more pronounced effect for the parental cells lines LNCaP and DU145, compared to their radioresistant counterparts (Figure 3F, S6F). Recent studies have demonstrated that overexpression of LEF1 might lead to cell resistance to tankyrase inhibition[27]. Noteworthy, DU145 RR cells express a significantly higher level of LEF1 as compared to the parental DU145 cells which contributes to XAV939 resistance (Figure S6G). Therefore changes in the phenotype of the radioresistant cell population during treatment are associated with deregulation of multiple intracellular signaling pathways, which can be attributed to the epigenetic and genetic alterations acquired by cells after irradiation.

***Alteration of histone methylation affects cell radioresistance and tumorigenicity***

Next, we determined whether epigenetic regulation of gene expression controlled by histone lysine methylation plays a role in the regulation of prostate cancer cell radioresistance. Our current studies suggest that irradiation induces activation of a number of proteins involved in the regulation of epigenetic modification of DNA and histones. As shown above, IPA-based interrogation of the gene expression data revealed histone H3 lysine

methyltransferase EZH2 as one of the most significantly upregulated transcriptional regulators in DU145-RR cells, compared to their parental counterparts (Figure S3C). To determine whether modulation of histone H3 methylation contributes to prostate cancer cell radioresistance, we examined the effect of inhibitors of lysine methyltransferases EZH2 and G9a, DZNep and BIX01294, respectively on the regulation of the viability and radiosensitivity of the parental and radioresistant DU145 cells. Noteworthy, DZNep is a broad spectrum methyltransferase inhibitor which affects both inhibitory and activating histone methylation marks, thus allowing a more comprehensive epigenetic resetting. Treatment with DZNep was significantly more potent for the inhibition of the viability of radioresistant LNCaP as compared to parental LNCaP cells and radioresistant DU145 cells as compared to parental DU145 cells (Figure 4A). In contrast, BIX01294 showed no significantly different effect in the radioresistant and parental LNCaP and DU145 cells (Figure S7A). Moreover, treatment of prostate cancer cells with DZNep decreased clonogenicity and radiosensitivity of the parental and radioresistant LNCaP and DU145 cells, with more pronounced effects on the radioresistant cell lines (Figure 4 BC, Figure S7B). In contrast to DZNep, BIX01294 had no significant inhibitory effects on the cell clonogenicity and radioresistance of the radioresistant and parental cell lines at the same range of concentrations (Figure 4 BC, Figure S7C). Analysis of the residual γ-H2A.X foci, 24 hours after irradiation, showed that pre-treatment of cells with DZNep significantly increased the number of unrepaired DSBs compared to the untreated cells. This effect was greater in the radioresistant cell lines than in the parental cells. Noteworthy, treatment of the cells with DZNep alone at a concentration of 1μM for 72h also led to significant accumulation of DNA DSBs as indicated by γ-H2A.X analysis (Figure 5A).

To understand the molecular mechanism of the more pronounced inhibitory effect of DZNep treatment on DU145-RR cells in comparison to their parental counterparts, DZNep was applied alone or in combination with X-irradiation, and the cells were analyzed by Western blotting for the activation of the apoptotic markers. Interestingly, DU145-RR cells

had a higher basal expression level of poly-ADP ribose polymerase (PARP), which is involved in DNA repair, genomic instability and transcription regulation, including prevention of the H3K4me3 demethylation[28]. Recent evidence points to the potential role of PARP in prostate cancer progression and therapy resistance, inferring that targeting of PAPR could serve as important therapeutic modality in hormone refractory prostate cancer[28]. In contrast to the parental DU145 cells, treatment of DU145-RR cells with DZNep induced caspase cascade and cleavage of PARP at Asp214, which mediates the apoptotic programs (Figure S8AB). Induction of the PARP cleavage in the DU145-RR and LNCaP-RR cells after treatment with DZNep was confirmed by fluorescent microscopy (Figure S8C).

An accumulation of DNA DSBs and the sensitivity of the cells to apoptosis can be attributed to disruption of intracellular redox balance. To determine if treatment with DZNep does disrupt redox balance in prostate cancer cells, gluthathione (GSH) and reactive oxygen species (ROS) levels were assessed by imaging cytometry or flow cytometry after incubation with monochlorobimane (mBCI) or 2',7'–dichlorofluorescin diacetate (DCFDA), respectively. Treatment with DZNep resulted in a decrease in GSH levels, and upregulation of ROS (Figure 5BC). The GSH level in DU145-RR cells was significantly more affected by the DZNep treatment as compared to the parental DU145 cells (Figure 5C). These results suggest that protective mechanisms of the radioresistant cells might rely on epigenetic regulation of genes involved in DNA repair and apoptosis.

Next we analyzed whether DZNep treatment can induce DNA DSBs and apoptotic signaling in prostate tumor specimens and primary prostate tumor cells. A freshly isolated lymph node biopsy of human hormone refractory prostate cancer (PT1) and a radical prostatectomy specimen (PT2) were dissected into pieces of approximately 3 × 3 mm, treated with 2 μM of DZNep for 24h, then irradiated with 4Gy of X-ray and fixed 24h after irradiation. Tissue culture was performed in serum-free, sphere forming cell medium. The presence of tumor cells in the tissue pieces was confirmed by staining with hematoxylin and

eosin (H&E) and by fluorescent immunostaining with anti-prostate specific membrane antigen (PSMA) and CK5/14 antibody (Figure 6A, Figure S9A). Microscopy analysis of the nuclear intensity of γ-H2A.X and cleaved PARP 24h after irradiation confirmed that inhibition of H3 methylation by DZNep led to an increase in DNA DSBs and induced activation of tumor cell apoptosis after *ex vivo* irradiation (Figure 6A). Primary cell cultures 312/13 and 311/13 were established from targeted needle biopsies of Gleason grade 7 tumors from the prostates of two patients who underwent radical prostatectomy at Castle Hill Hospital, Cottingham, UK (kindly provided by Prof. Norman Maitland, University of York). For these experimental models, only combination of DZNep treatment with 4 Gy irradiation led to significant increase in the nuclear γ-H2A.X intensity 24h after irradiation compared to untreated control cells, whereas no significant difference was seen between control cells and irradiated cells without DZNep treatment (Figure S9B).

In comparison, treatment of the immortalized, non-tumorigenic cell line RWPE1 with DZNep did not lead to a significant increase in residual DNA damage as compared to the treatment by irradiation alone suggesting that radiosensitizing effect of DZNep can be more pronounced in malignant cells as compared to normal cells (Figure S9C).

Next we addressed the question of whether DZNep inhibition directly affects expression of stem cell markers such as ALDH1A1. Western blot analysis revealed that treatment of prostate cancer cells with DZNep led to an inhibition of EZH2 and ALDH1A1 and to a decrease in tri-methylation of lysine residue K36 in histone H3 (Figure 6B, Figure S9D). Inhibition of ALDH1A1 expression was also observed in DU145 cells pretreated with DZNep and subsequently irradiated with 4Gy of X-ray. These findings suggest that this inhibitor can be used to prevent tumor cell reprogramming induced by irradiation (Figure S9EF).

In accordance with the results of gene expression analysis and our previous findings[16], small interfering (si) RNA-mediated inhibition of β-catenin expression decreases expression

of EZH2 and ALDH1A1 in prostate cancer cells, and DZNep treatment has an additive effect on β-catenin knockdown with regard to EZH2 and ALDH1A1 expression (Figure S10A). These results suggest a link between the activation of WNT/β-catenin signaling pathway after cell irradiation and irradiation-induced epigenetic changes. Strikingly, *ALDH1A1* and *EZH2* genes are frequently co-expressed with *CTNNB1* (β-catenin) in prostate tumor specimens (Figure S10B). Moreover, a gene signature, which includes expression of *ALDH1A1* and *EZH2* correlated with reduced disease-free survival in patients with prostate cancer, as suggested the analysis of the provisional TCGA data set extracted from cBioPortal for Cancer Genomics (Figure S10C).

To analyze whether inhibition of the H3 methylation by DZNep can affect cell tumorigenicity after irradiation, we compared the relative *in vivo* growth of DU145 and DU145-RR cells after *in vitro* pre-treatment with DZNep alone, or in combination with irradiation. The cells were treated with 1μM of DZNep or with DMSO as a control for 72h, irradiated with 6Gy of X-ray or left non-irradiated, embedded in matrigel and injected subcutaneously into NMRI nu/nu mice. Animals alive and tumor-free at the end of the observation period (77 days) were defined as long-term survivors. In contrast to the parental cells, DU145-RR cells pre-treated with DZNep had a significantly lower relative tumor growth rate and tumor take than control cells, and the inhibitory effect of the DZNep treatment on DU145-RR cell tumorigenicity was significantly increased after irradiation leading to complete inhibition of DU145-RR cell tumorigenicity (Figure 6CD).

**Discussion**

Radiation therapy is one of the most effective treatments for cancer and is a potentially curative treatment option for patients with clinically localized prostate carcinoma[29]. Recent discoveries have provided compelling evidence that cancer stem cell population (CSC) within each individual tumor is a key contributor of radiotherapy failure, regardless of whether this

population is transient or stable[30]. Therefore, tumors can only be cured if all CSCs are targeted, or when the host is able to inactivate those CSC surviving anti-cancer treatment[7]. However, development of therapeutic agents eradicating CSCs remains challenging due to the high diversity and plasticity of CSC phenotypes. Recent advances in DNA sequencing allowing global analysis of genetic landscape in individual tumor cells revealed a high heterogeneity of different subclones within the same tumor specimens and has provided an insight into the subclonal evolution, suggesting that CSC and clonal evolution models are not mutually exclusive[15, 31]. Furthermore, evolved CSCs which survive after chemo- or radiotherapy might confer treatment resistance. By using CGH analysis, we revealed multiple genomic alterations and pronounced changes in the global gene expression profiling in prostate cancer cells which have been irradiated with multiple doses of X-rays. Therefore, we hypothesized that irradiation-induced genomic instability might lead to the evolution of the tumor-initiating populations that change their phenotypic features during the course of irradiation.

In our previous study we found that prostate tumor initiating cells with high aldehyde dehydrogenase activity ($ALDH^+$ cells) were more radioresistant than $ALDH^-$ cells, and inhibition of ALDH activity radiosensitizes prostate cancer cells[16]. In the present study we have addressed the question whether tumor initiating cells with acquired radioresistance can also be defined by a high ALDH activity. Surprisingly, although RR $ALDH^+$ population possesses higher clonogenic and tumorigenic potential compared to RR $ALDH^-$ cells, these two populations cannot be distinguished by either their radioresistance properties or by the activation of WNT/β-catenin signaling pathway and migratory potential. These results indicate that the radioresistant tumor initiating cell populations undergo a phenotypic switching during the course of radiotherapy by analogy with a lineage switch in leukemia patients after chemotherapy[32-34], and functional changes in ovarian and prostate CSCs following paclitaxel or docetaxel treatment[20, 35]. Furthermore, recent data suggest that

ALDH1A1 expression is predictive of poor prognosis in hormone-naïve prostate cancer patients. In contrast, in patients with castration-resistant disease, ALDH1A1 expression does not correlate with clinical outcome[25].

The previously published studies suggested that phenotypic plasticity of tumor initiating cells might be associated not only with certain genetic but also with epigenetic changes, which can be essential for cell tumorigenicity and therapy resistance[15, 36]. Indeed, accumulating experimental evidence suggests that tumor cell dedifferentiation, based on the induced reprogramming of cancer cells is analogous to the reprogramming of the differentiated somatic cells into pluripotent cells[37]. Therefore, efficient anti-cancer treatment must eradicate both CSCs and the tumor bulk to prevent tumor cell de-differentiation. The populations of tumor cells with salient features of CSCs can be induced *in vivo* in response to the different microenvironmental stimuli which include hypoxia, genetic alterations which trigger epithelial to mesenchymal transition (EMT) as well as cancer therapies[26, 37, 38]. In agreement with this, recently published data showed that irradiation may induce reprogramming of differentiated breast and hepatocellular carcinoma cells[39-41]. Consistent with these findings, we have previously shown that fractions of the cells positive for CSC markers, e.g. ABCG2, CD133, ALDH activity were significantly enriched after fractionated irradiation that can be potentially attributed to cell selection as well as to cell induction mechanisms including both, accelerated proliferation and reprogramming[16, 39, 40].

Notably, our data revealed that a single 4 Gy irradiation induces a prolonged effect on the clonogenic potential and expression of both CSC and EMT markers, which lasts for more than 6 weeks. The dynamics of protein expression after cell irradiation can reflect a continuous process, resulting in consequent changes of cell phenotype and functional properties, and resembling the reprogramming process of somatic cells. Indeed we have shown that irradiation induces methylation of H3K4 and H3K36, which is a hallmark of the reactivated transcription of the epigenetically silenced target genes. In support of the

hypothesis that irradiation can induce prostate tumor cell populations with CSC features, our study shows that irradiation of $ALDH^-$ prostate carcinoma cells leads to an induction of an $ALDH^+$ cell subset within this population. This mechanism can potentially contribute to the enrichment of the cells with CSC phenotype after irradiation.

Heritable epigenetic regulation of gene expression which includes changes in DNA methylation and histone posttranslational modification plays an important role in the regulation of tumor response to the treatment. Histone modification patterns have been correlated to tumor recurrence in patients with prostate cancer[42]. In support of the hypothesis that irradiation-induced epigenetic changes can regulate tumor response to therapy, we found that expression of the *ALDH1A1* gene, which is indicative of prostate cancer cells with increased tumorigenicity and radioresistance, is regulated by the irradiation-induced epigenetic changes. Our previous studies demonstrated that *ALDH1A1* gene expression is directly activated by the β-catenin/TCF transcriptional complex[16]. Using a ChIP assay specific for the β-catenin/TCF binding sites of the *ALDH1A1* gene promoter, we revealed that irradiation induced tri-methylation of Lys 36 in histone H3 (H3K36me3) on the *ALDH1A1* promoter. This modification has been associated with activation of *ALDH1A1* gene transcription. Our studies suggest that irradiation induced expression of the different genes involved in the regulation of epigenetic modifications including expression of the lysine methyltransferase EZH2. Overexpression of EZH2 has been associated with a number of cancers, including prostate, breast cancer and melanoma[43-46]. Recent studies revealed that EZH2 enhances WNT/β-catenin mediated gene transactivation[47]. Moreover, expression of *EZH2* was inhibited by siRNA-mediated knockdown of β-catenin, suggesting a direct link between irradiation-induced activation of the WNT/β-catenin signaling pathway and epigenetic reprogramming of the tumor cells. In accordance with this observation, expression of *ALDH1A1* and *EZH2* genes has a tendency toward co-occurrence with expression of the *CTNNB1* (β-catenin) gene in prostate tumor specimens[48]. The chemical inhibition of EZH2

with DZNep, which acts as a broad methyltransferase inhibitor resulted in the downregulation of *ALDH1A1* expression and led to a significant increase in cell radiosensitivity and inhibition of the tumorigenic properties. A compound such as DZNep decreases H3K27me3 and H3K9me2 repressive methylation mediated by EZH2 as well as the active histone mark H3K4me3 and H3K36me3, therefore preventing a broad epigenetic resetting of the tumor cells[49]. Noteworthy, all-trans retinoid acid (ATRA), which is the only chemical drug in clinical use for tumor cell differentiation and is an inhibitor of ALDH activity, was recently shown to reduce the proliferation of prostate cancer DU145 cells, through downregulation of EZH2-mediated methylation of the *HOXB13* gene which encodes Hoxb13 anti-proliferative transcription factor[50]. Several studies have demonstrated that the level of EZH2 expression is positively correlated with prostate cancer aggressiveness, and EZH2 is not only overexpressed in metastatic prostate cancer but also in the localized cancers with a high risk of recurrence after radical prostatectomy[22, 46, 51, 52]. A high EZH2 expression in esophageal squamous cell carcinoma and rectal cancer was significantly correlated with the lack of clinical complete response to chemoradiotherapy[53, 54]. Another study has demonstrated that EZH2 protects glioma stem cells from irradiation-induced cell death[55]. Taken together, these finding demonstrate that EZH2 bears significant potential to serve as a diagnostic and prognostic marker for prostate cancer and other cancers and as a therapeutic target for tumor radiosensitization. In support of this, recent clinical studies of the various epigenetic inhibitors including EZH2 inhibitors EPZ-6438 and CPI-1205 for the treatment of patients with advanced solid tumors or lymphomas (ClinicalTrials.gov identifier NCT01897571 and NCT02395601), as well as the inhibitors of histone deacetylases (HDAC), which are already approved for clinical use or currently being clinically investigated, are paving the way to improved effectiveness of cancer treatment by the inhibition of tumor cell reprogramming.

This study is, to our best knowledge, the first investigation which demonstrates that radioresistant populations within prostate cancer cells undergo a phenotypic switch during the

course of irradiation, rather than being selected from the preexisting cell pool. We revealed that irradiation drives histone modifications on the promoter sequence of *ALDH1A1* genes, which regulate cancer cell tumorigenicity and radioresistance. Our findings demonstrated that treatment of tumor cells with DZNep resulted in a significant increase in DNA damage, cell apoptosis and radiosensitivity, and cells with a higher radioresistance are more sensitive to DZNep treatment.

Future research are needed to validate our findings by using additional experiments on primary cultures and tumor biopsies and by combination of the drug with radiation therapy in human prostate cancer xenograft mouse models. Our data suggest that compounds such as DZNep that inhibit EZH2 and prevents a broad resetting of histone methylation marks may be useful as epigenetic co-therapy to prevent tumor cell reprogramming into more aggressive and therapy resistant state (Figure 7).

**Acknowledgements**

We thank Vasyl Lukiyanchuk for assistance with analysis of the gene expression data and Celigo imaging, Dr. Annette Linge for help with pathological examination of the tumor tissues and Dr. Steffen Löck for help with statistical analysis. This work was supported by BMBF grants (ZIK OncoRay) to AD, MB, MK and by the German Cancer Consortium (DKTK) Partnersite Dresden.

**Author contribution**

CP, MC, LH, FT and AD performed, analyzed, and interpreted experiments. IK and KM provided ideas and experimental support. MB and MK, together with AD developed the CSC biomarkers for radiation oncology program, in which context this study was performed and regularly discussed. MPW, EAS, GDT, GBB, NJM, FMF, VN conceived of the study and provided the materials. MT and MM performed pathological examination of the tumor

specimens. MB, MK, IK, CP, BK and MC performed review of the manuscript. BK and ES performed comparative genome hybridization analysis. AD supervised the experiments, analyzed the results and wrote the manuscript.

**References:**

1. Ferlay J, Steliarova-Foucher E, Lortet-Tieulent J, et al. Cancer incidence and mortality patterns in Europe: estimates for 40 countries in 2012. Eur J Cancer. 2013;49: 1374-1403.
2. Ghotra VP, Geldof AA, Danen EH. Targeted radiosensitization in prostate cancer. Curr Pharm Des. 2013;19: 2819-2828.
3. Rukstalis DB. Treatment options after failure of radiation therapy-a review. Rev Urol. 2002;4 Suppl 2: S12-17.
4. Zietman AL, Bae K, Slater JD, et al. Randomized trial comparing conventional-dose with high-dose conformal radiation therapy in early-stage adenocarcinoma of the prostate: long-term results from proton radiation oncology group/american college of radiology 95-09. J Clin Oncol. 2010;28: 1106-1111.
5. Pahlajani N, Ruth KJ, Buyyounouski MK, et al. Radiotherapy doses of 80 Gy and higher are associated with lower mortality in men with Gleason score 8 to 10 prostate cancer. Int J Radiat Oncol Biol Phys. 2012;82: 1949-1956.
6. Johansson S, Astrom L, Sandin F, Isacsson U, Montelius A, Turesson I. Hypofractionated proton boost combined with external beam radiotherapy for treatment of localized prostate cancer. Prostate Cancer. 2012;2012: 654861.
7. Baumann M, Krause M, Hill R. Exploring the role of cancer stem cells in radioresistance. Nat Rev Cancer. 2008;8: 545-554.
8. Brunner TB, Kunz-Schughart LA, Grosse-Gehling P, Baumann M. Cancer stem cells as a predictive factor in radiotherapy. Semin Radiat Oncol. 2012;22: 151-174.
9. Pajonk F, Vlashi E, McBride WH. Radiation resistance of cancer stem cells: the 4 R's of radiobiology revisited. Stem Cells. 2010;28: 639-648.
10. O'Brien CA, Kreso A, Jamieson CH. Cancer stem cells and self-renewal. Clin Cancer Res. 2010;16: 3113-3120.
11. Baumann M, Dubois W, Suit HD. Response of human squamous cell carcinoma xenografts of different sizes to irradiation: relationship of clonogenic cells, cellular radiation sensitivity in vivo, and tumor rescuing units. Radiat Res. 1990;123: 325-330.
12. Hill RP, Milas L. The proportion of stem cells in murine tumors. Int J Radiat Oncol Biol Phys. 1989;16: 513-518.
13. Butof R, Dubrovska A, Baumann M. Clinical perspectives of cancer stem cell research in radiation oncology. Radiother Oncol. 2013;108: 388-396.
14. Linge A LS, Gudziol V, Nowak A, Lohaus F, von Neubeck C, Jütz M, Abdollahi A, Debus J, Tinhofer I, Budach V, Gkika E, Stuschke M, Balermpas P, Rödel C, Avlar M, Grosu AL, Bayer C, Belka C, Pigorsch S, Combs SE, Mönnich D, Zips D, Buchholz F, Aust DE, Baretton GB, Thames H, Dubrovska A, Alsner J, Overgaard J, Baumann M, Krause M. Low cancer stem cell marker expression and low hypoxia identify good prognosis subgroup for loco-regional control after postoperative radiochemotherapy in HPV16 DNA negative HNSCC: Results from a multicenter biomarker study of the German Cancer Consortium Radiation Oncology Group (DKTK-ROG). Clin Cancer Res. 2016 Jan 11. pii: clincanres.1990.2015.
15. Kreso A, Dick JE. Evolution of the cancer stem cell model. Cell Stem Cell. 2014;14: 275-291.
16. Cojoc M, Peitzsch C, Kurth I, et al. Aldehyde dehydrogenase is regulated by Beta-catenin/TCF and promotes radioresistance in prostate cancer progenitor cells. Cancer Res. 2015.

17. Frame FM, Pellacani D, Collins AT, et al. HDAC inhibitor confers radiosensitivity to prostate stem-like cells. Br J Cancer. 2013;109: 3023-3033.
18. Franken NA, Rodermond HM, Stap J, Haveman J, van Bree C. Clonogenic assay of cells in vitro. Nat Protoc. 2006;1: 2315-2319.
19. van den Hoogen C, van der Horst G, Cheung H, et al. High aldehyde dehydrogenase activity identifies tumor-initiating and metastasis-initiating cells in human prostate cancer. Cancer Res. 2010;70: 5163-5173.
20. Dubrovska A, Elliott J, Salamone RJ, et al. Combination therapy targeting both tumor-initiating and differentiated cell populations in prostate carcinoma. Clin Cancer Res. 2010;16: 5692-5702.
21. McDonald OG, Wu H, Timp W, Doi A, Feinberg AP. Genome-scale epigenetic reprogramming during epithelial-to-mesenchymal transition. Nat Struct Mol Biol. 2011;18: 867-874.
22. Berezovska OP, Glinskii AB, Yang Z, Li XM, Hoffman RM, Glinsky GV. Essential role for activation of the Polycomb group (PcG) protein chromatin silencing pathway in metastatic prostate cancer. Cell Cycle. 2006;5: 1886-1901.
23. Sharma A, Singh K, Almasan A. Histone H2AX phosphorylation: a marker for DNA damage. Methods Mol Biol. 2012;920: 613-626.
24. Menegakis A, von Neubeck C, Yaromina A, et al. gammaH2AX assay in ex vivo irradiated tumour specimens: A novel method to determine tumour radiation sensitivity in patient-derived material. Radiother Oncol. 2015.
25. Le Magnen C, Bubendorf L, Rentsch CA, et al. Characterization and clinical relevance of ALDHbright populations in prostate cancer. Clin Cancer Res. 2013;19: 5361-5371.
26. Nieto MA. Epithelial plasticity: a common theme in embryonic and cancer cells. Science. 2013;342: 1234850.
27. de la Roche M, Ibrahim AE, Mieszczanek J, Bienz M. LEF1 and B9L shield beta-catenin from inactivation by Axin, desensitizing colorectal cancer cells to tankyrase inhibitors. Cancer Res. 2014;74: 1495-1505.
28. Deshmukh D, Qiu Y. Role of PARP-1 in prostate cancer. Am J Clin Exp Urol. 2015;3: 1-12.
29. Baumann M, Krause M, Overgaard J, et al. Radiation oncology in the era of precision medicine. Nat Rev Cancer, 2016 in press
30. Kuhlmann JD, Hein L, Kurth I, Wimberger P, Dubrovska A. Targeting cancer stem cells: promises and challenges. Anticancer Agents Med Chem. 2015.
31. Peitzsch C, Kurth I, Kunz-Schughart L, Baumann M, Dubrovska A. Discovery of the cancer stem cell related determinants of radioresistance. Radiother Oncol. 2013;108: 378-387.
32. Mullighan CG, Phillips LA, Su X, et al. Genomic analysis of the clonal origins of relapsed acute lymphoblastic leukemia. Science. 2008;322: 1377-1380.
33. Ding L, Ley TJ, Larson DE, et al. Clonal evolution in relapsed acute myeloid leukaemia revealed by whole-genome sequencing. Nature. 2012;481: 506-510.
34. Stass S, Mirro J, Melvin S, Pui CH, Murphy SB, Williams D. Lineage switch in acute leukemia. Blood. 1984;64: 701-706.
35. Craveiro V, Yang-Hartwich Y, Holmberg JC, et al. Phenotypic modifications in ovarian cancer stem cells following Paclitaxel treatment. Cancer Med. 2013;2: 751-762.
36. Meacham CE, Morrison SJ. Tumour heterogeneity and cancer cell plasticity. Nature. 2013;501: 328-337.
37. Tang DG. Understanding cancer stem cell heterogeneity and plasticity. Cell Res. 2012;22: 457-472.
38. Peitzsch C, Perrin R, Hill RP, Dubrovska A, Kurth I. Hypoxia as a biomarker for radioresistant cancer stem cells. Int J Radiat Biol. 2014;90: 636-652.
39. Lagadec C, Vlashi E, Della Donna L, Dekmezian C, Pajonk F. Radiation-induced reprogramming of breast cancer cells. Stem Cells. 2012;30: 833-844.
40. Wang Y, Li W, Patel SS, et al. Blocking the formation of radiation-induced breast cancer stem cells. Oncotarget. 2014;5: 3743-3755.

41. Ghisolfi L, Keates AC, Hu X, Lee DK, Li CJ. Ionizing radiation induces stemness in cancer cells. PLoS One. 2012;7: e43628.
42. Seligson DB, Horvath S, Shi T, et al. Global histone modification patterns predict risk of prostate cancer recurrence. Nature. 2005;435: 1262-1266.
43. Yang YA, Yu J. EZH2, an epigenetic driver of prostate cancer. Protein Cell. 2013;4: 331-341.
44. Bracken AP, Pasini D, Capra M, Prosperini E, Colli E, Helin K. EZH2 is downstream of the pRB-E2F pathway, essential for proliferation and amplified in cancer. EMBO J. 2003;22: 5323-5335.
45. Visser HP, Gunster MJ, Kluin-Nelemans HC, et al. The Polycomb group protein EZH2 is upregulated in proliferating, cultured human mantle cell lymphoma. Br J Haematol. 2001;112: 950-958.
46. Varambally S, Dhanasekaran SM, Zhou M, et al. The polycomb group protein EZH2 is involved in progression of prostate cancer. Nature. 2002;419: 624-629.
47. Jung HY, Jun S, Lee M, et al. PAF and EZH2 induce Wnt/beta-catenin signaling hyperactivation. Mol Cell. 2013;52: 193-205.
48. Taylor BS, Schultz N, Hieronymus H, et al. Integrative genomic profiling of human prostate cancer. Cancer Cell. 2010;18: 11-22.
49. He S, Wang J, Kato K, et al. Inhibition of histone methylation arrests ongoing graft-versus-host disease in mice by selectively inducing apoptosis of alloreactive effector T cells. Blood. 2012;119: 1274-1282.
50. Liu Z, Ren G, Shangguan C, et al. ATRA inhibits the proliferation of DU145 prostate cancer cells through reducing the methylation level of HOXB13 gene. PLoS One. 2012;7: e40943.
51. Hoffmann MJ, Engers R, Florl AR, Otte AP, Muller M, Schulz WA. Expression changes in EZH2, but not in BMI-1, SIRT1, DNMT1 or DNMT3B are associated with DNA methylation changes in prostate cancer. Cancer Biol Ther. 2007;6: 1403-1412.
52. Saramaki OR, Tammela TL, Martikainen PM, Vessella RL, Visakorpi T. The gene for polycomb group protein enhancer of zeste homolog 2 (EZH2) is amplified in late-stage prostate cancer. Genes Chromosomes Cancer. 2006;45: 639-645.
53. He LR, Liu MZ, Li BK, et al. High expression of EZH2 is associated with tumor aggressiveness and poor prognosis in patients with esophageal squamous cell carcinoma treated with definitive chemoradiotherapy. Int J Cancer. 2010;127: 138-147.
54. Meng X, Huang Z, Wang R, et al. The prognostic role of EZH2 expression in rectal cancer patients treated with neoadjuvant chemoradiotherapy. Radiat Oncol. 2014;9: 188.
55. Kim SH, Joshi K, Ezhilarasan R, et al. EZH2 Protects Glioma Stem Cells from Radiation-Induced Cell Death in a MELK/FOXM1-Dependent Manner. Stem Cell Reports. 2015;4: 226-238.

## Figure legends

**Figure 1. Analysis of the time-dependent effects of irradiation on the properties of prostate cancer cells. A**, The delayed effect of X-ray irradiation on the expression of the stem cell and EMT markers. After irradiated with 4 Gy of X-ray, the lysates of DU145 and LNCaP cells were prepared at the indicated time points during 6 weeks after irradiation and analyzed by Western blotting; NI - non-irradiated cells. The accompanying graphs display the densitometry-based analysis of the western blot data. **B**, Flow cytometry analysis of the ALDH activity in DU145 and DU145-RR cells within 6 weeks after irradiation with 4Gy of

X-ray. Error bars represent S.E.M.; n=4. **C**, The colony forming properties of DU145 cells and DU145-RR cells were analyzed within 6 weeks after the last irradiation; Error bars represent S.E.M; Error bars represent S.E.M.; n=3. **D**, Induction of the $ALDH^+$ cell population after irradiation of $ALDH^+$ and $ALDH^-$ cell subsets. FACS sorted $ALDH^+$ and $ALDH^-$ cells were plated in a 6 well plate and irradiated with 4Gy 18 hours later. Irradiation with 4Gy was repeated at day 7 after first irradiation. The cells were analyzed at day 14 by flow cytometry. Error bars represent S.E.M; n=3.

**Figure 2. Epigenetic alterations in the irradiated prostate cancer cells. A**, Gene expression profiling of the DU145 parental and DU145-RR cells and FACS-isolated $ALDH^+$ and $ALDH^-$ cell populations revealed a number of genes involved in the epigenetic regulation of protein expression through DNA and histone modifications. **B**, GSEA enrichment analysis for the genes upregulated in DU145-RR as compared to DU145 cells. The 'Hallmark epithelial mesenchymal transition' gene set includes genes defining epithelial-mesenchymal transition, as in wound healing, fibrosis and metastasis. The 'Mikkelsen MEF LCP with H3K4me3' gene set includes genes with low-CpG-density promoters (LCP) bearing a tri-methylation mark at H3K4 (H3K4me3) in MEF cells (embryonic fibroblasts). **C**, Irradiation induces long-lasting changes in H3K4, H3K36 and H3K27 tri-methylation. DU145 and LNCaP cells were irradiated with 4 Gy of X-ray, and the lysates of cells were prepared at the indicated time points during 6 weeks after irradiation and analyzed by Western blotting; NI - non-irradiated cells. **D**, Analysis of H3K4 and H3K36 methylation in response to irradiation. Densitometric analysis of the protein immunoblots is shown in the accompanying graph. The level of H3K4 and H3K36 methylation was normalized to the total H3 level. Error bars represent S.E.M; n=3; *, $p < 0.05$. **E**, The results of ChIP analysis showed that irradiation induces a H3K36me3 transcription activation mark on *ALDH1A1* promoter within two core β-catenin/TCF binding sites (i) and [22] as described earlier[16]. Error bars represent S.E.M; n=3; *, $p < 0.05$. **F**, The results of the luciferase reporter assay where luciferase gene expression is

regulated by an endogenous *ALDH1A1* gene promoter showed that *ALDH1A1* transcription is significantly increased in DU145-RR and LNCaP-RR cells as compared to the parental cell lines. Error bars represent S. E. M; n≥3; *, $p < 0.05$.

**Figure 3. Irradiation-induced plasticity of the mechanisms of radioresistance in prostate cancer cells. A**, Clonogenic cell survival assay showing that, in contrast to $ALDH^+$ and $ALDH^-$ cell populations isolated from parental DU145 cells, DU145-RR $ALDH^+$ and DU145-RR $ALDH^-$ cells do not differ in their radioresistance properties. Error bars represent S.E.M; n≥5. **B**, Immunofluorescence analysis of the residual γ-H2A.X foci in $ALDH1A3^+$ and $ALDH1A3^-$ cells 24h after irradiation with 4Gy of X-ray. Error bars represent S.E.M; n=5; *, $p < 0.05$. **C**, Comparative gene expression profiling of $ALDH^+$ and $ALDH^-$ cell populations in the parental DU145 and DU145-RR cells. Venn diagrams show an overlap in the sets of genes differently regulated between DU145 and DU145-RR cells in comparison to DU145 $ALDH^+$ and DU145 $ALDH^-$ cells or to DU145-RR $ALDH^+$ and DU145-RR $ALDH^-$ cells. PANTHER analysis was used to identify the pathways overrepresented among the genes that are differentially regulated in DU145 $ALDH^+$ and DU145 $ALDH^-$ cells and DU145-RR $ALDH^+$ and DU145-RR $ALDH^-$ cells. **D**, Hierarchical clustering analysis of the WNT signaling pathway genes differentially regulated between DU145 and DU145-RR, DU145 $ALDH^+$ and DU145 $ALDH^-$ as well as DU145-RR $ALDH^+$ and DU145-RR $ALDH^-$. **E**, Immunofluorescence analysis of the intracellular distribution of β-catenin in DU145 RR $ALDH^+$ and DU145 RR $ALDH^-$ cell subsets. Error bars represent S.E.M; n=2. **F**, The inhibition of WNT signaling pathway with XAV939 inhibitor does not affect radiosensitivity of LNCaP-RR and DU145-RR cells. The cells were serum starved in DMEM with 3% FBS for 24 h followed by treatment with XAV939 antagonist at concentration 1μM for 72h. Error bars represent S.E.M; n≥3; *, $p < 0.01$.

**Figure 4. Inhibition of the histone methylation activity decreases prostate cancer cell viability and radioresistance. A**, DZNep, a global histone methylation inhibitor, is

more potent for the inhibition of viability of LNCaP-RR and DU145–RR cells as compared to their parental counterparts. $IC_{50}$ values were determined after 24 h ($n \geq 3$) and 72 h ($n \geq 2$) of treatment with the drugs. **B**, Plating efficacy of the LNCaP, LNCaP-RR, DU145 and DU145-RR cells pre-treated with DZNep or BIX-01294 at the different concentrations for 72h. Error bars represent S.E.M; $n \geq 3$; *, $p < 0.05$. **C**, Cells were pre-treated with DZNep or BIX-01294 at the different concentrations in DMEM with 3% FBS for 72h and their susceptibility to X-ray irradiation was evaluated by clonogenic cell survival assay; Error bars represent S.E. M.*, $p < 0.05$.

**Figure 5. Mechanisms of DZNep-mediated prostate cancer cell radiosensitization.** **A**, Analysis of γH2A.X foci in cells treated with DZNep at a concentration of 1 μM for 72h alone or in combination with 4Gy of X-ray irradiation 48h after start of DZNep treatment. Residual γH2A.X foci were analyzed 24 hours after irradiation. Error bars represent S.E.M; n=3; *, $p < 0.05$; **, $p < 0.01$. **B**, Analysis of reactive oxygen (ROS) level after treatment of cells with DZNep at a concentration of 1 μM for 72h. Cells treated with DMSO were used as control. Error bars represent S.E.M; n=3; *, $p < 0.05$. **C**, Measurement of the glutathione (GSH) levels in the cells pretreated with DMSO or DZNep at a concentration of 1 μM for 72h by incubation with monochlorobimane (mBCI) and Celigo cytometry. Error bars represent S.E.M; n=8; *, $p < 0.05$.

**Figure 6. Regulation of histone methylation impacts prostate cancer cell tumorigenicity. A**, Analysis of apoptosis induction and γH2A.X increase in the specimens of node metastasis of prostate tumor (PT1) and radical prostatectomy (PT2), which were treated with 4 Gy of X-ray alone or in combination with 2 μM of DZNep given for 48 h. The tissues were fixed 24h after irradiation. Error bars represent S.E.M. **B**, Western blot analysis of the parental and radioresistant LNCaP and DU145 cell lines treated with DZNep or BIX-01294 at a concentration of 1 μM for 72h. Densitometric analysis of the protein immunoblots is shown in the accompanying graph. Error bars represent S.E.M **C**, Tumor uptake rates in mice

injected with $5x10^4$ DU145 or DU145-RR cells. The cells were pretreated with DZNep before injection at a concentration 1 μM for 72h alone or in combination with 6Gy of X-ray irradiation given 48h after the start of DZNep treatment. Cells treated with DMSO and sham-irradiation were used as a control; the p-value was calculated using log-rank (Mantel-Cox) test. **D**, Relative tumor growth of DU145 and DU145-RR cells treated as indicated. Error bars represent S.E.M; *, $p < 0.05$.

**Figure 7. Proposed model of regulation of prostate cancer cell radioresistance by epigenetic mechanisms.** Irradiation-mediated activation of the WNT/β-catenin signaling pathway leads to cell reprogramming and cancer stem cell plasticity. Inhibition of the global histone methylation by DZNep results in impaired DNA reparation, induction of apoptosis and increase of cell radiosensitivity.

Figure 1

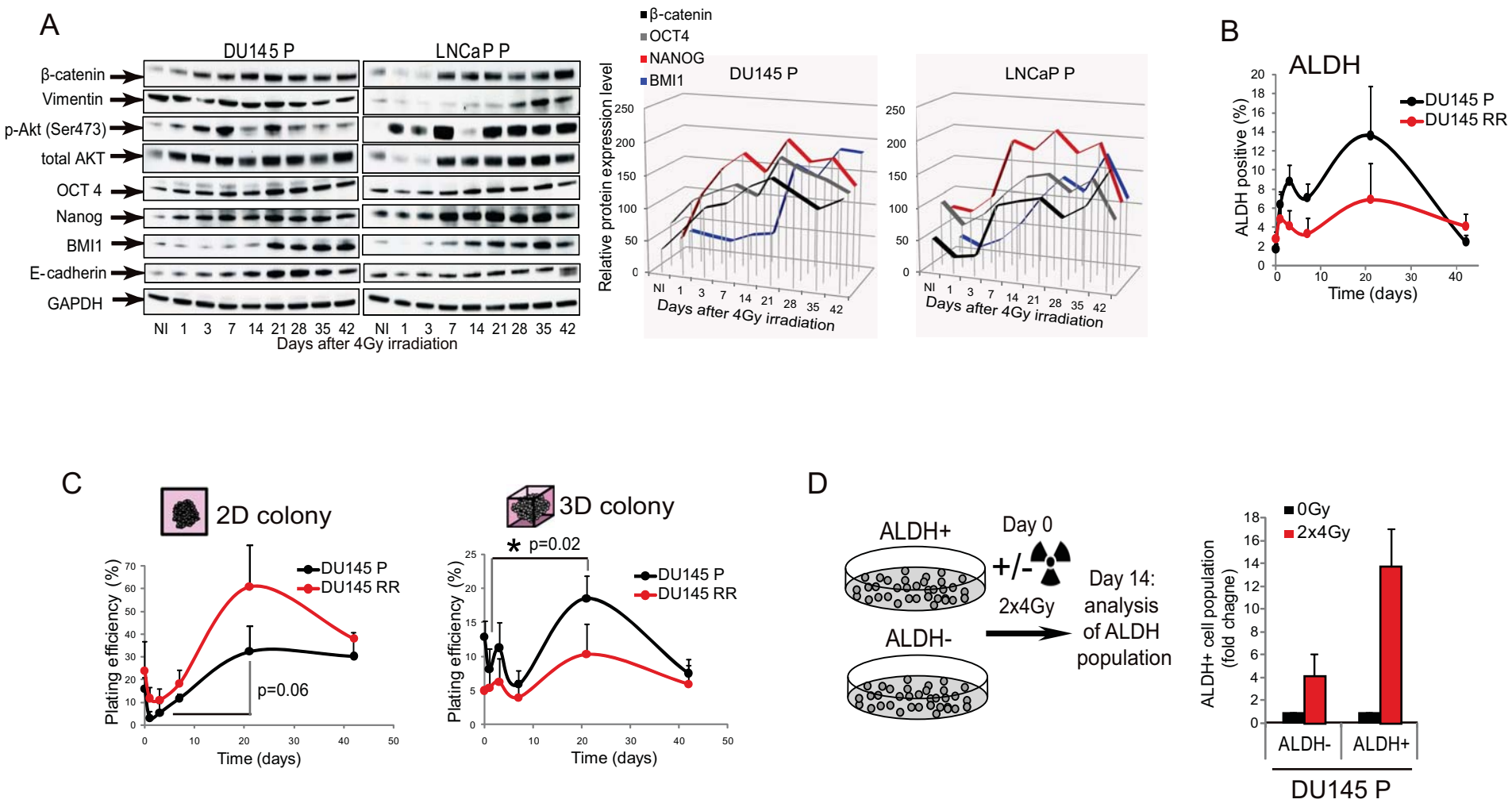

Figure 2

A

DU145 RR vs. DU145 P

| | fold change | p-value |
|---|---|---|
| ASMTL | | 0.003 |
| DNMT3B | | 0.000 |
| DOT1L | | 0.031 |
| EZH2 | | 0.045 |
| HDAC1 | | 0.009 |
| HDAC11 | | 0.008 |
| HDAC2 | | 0.013 |
| HDAC5 | | 0.007 |
| HDAC6 | | 0.006 |
| HDAC8 | | 0.006 |
| HEMK1 | | 0.001 |
| LRTOMT | | 0.000 |
| METTL15 | | 0.005 |
| METTL21A | | 0.020 |
| METTL25 | | 0.021 |
| METTL2A | | 0.005 |
| METTL3 | | 0.000 |
| NSD1 | | 0.012 |
| PCMTD2 | | 0.004 |
| PNMT | | 0.019 |
| SET | | 0.008 |
| SETD3 | | 0.003 |
| SETD5 | | 0.001 |
| SETD5-AS1 | | 0.006 |
| SETD5-AS1 | | 0.030 |
| SETD6 | | 0.006 |
| SETD8 | | 0.002 |
| SETD8 | | 0.009 |
| SHMT1 | | 0.001 |
| SMYD2 | | 0.001 |
| SUV39H2 | | 0.011 |
| TPMT | | 0.010 |

DU145 P ALDH+ vs. ALDH-

| | fold change | p-value |
|---|---|---|
| HDAC1 | | 0.014 |
| HDAC11 | | 0.008 |
| HDAC2 | | 0.004 |
| HDAC5 | | 0.007 |
| HDAC6 | | 0.006 |
| HDAC8 | | 0.005 |
| METTL15 | | 0.019 |
| MLL | | 0.018 |
| MLL5 | | 0.004 |
| MLLT11 | | 0.018 |
| SUV420H2 | | 0.020 |

B

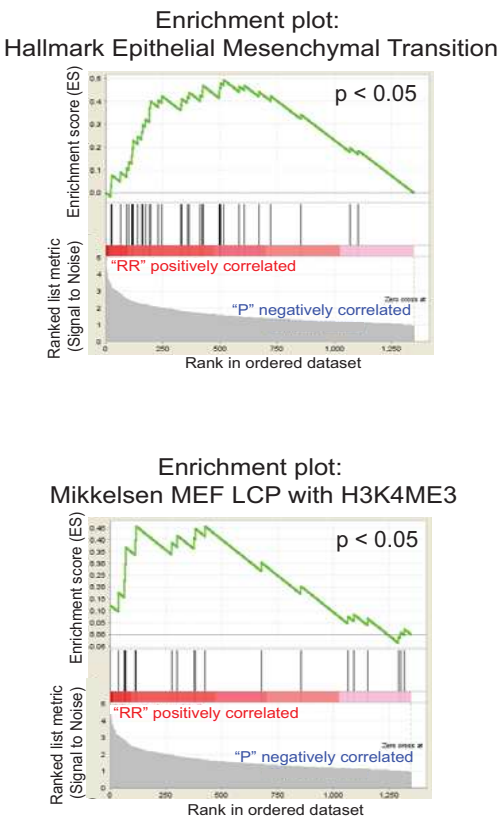


C

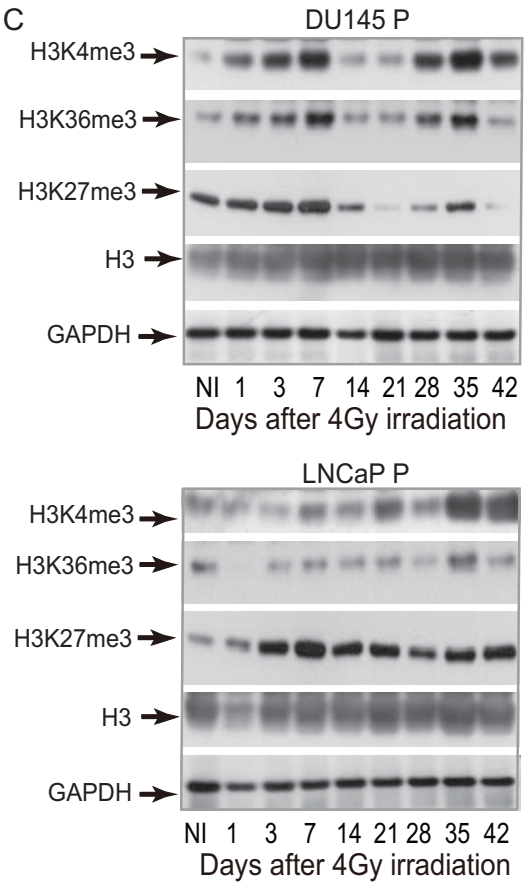


D

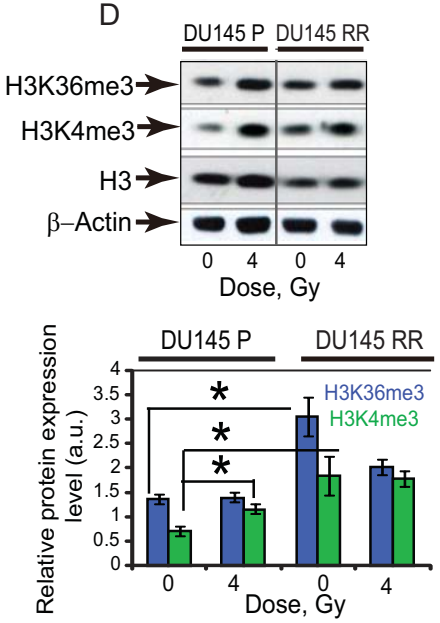


E

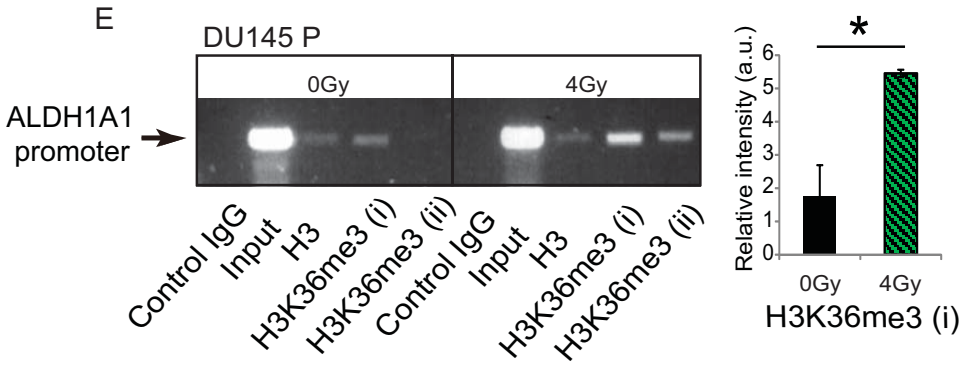


F

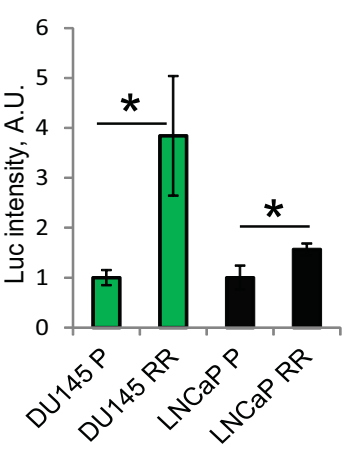

Figure 3

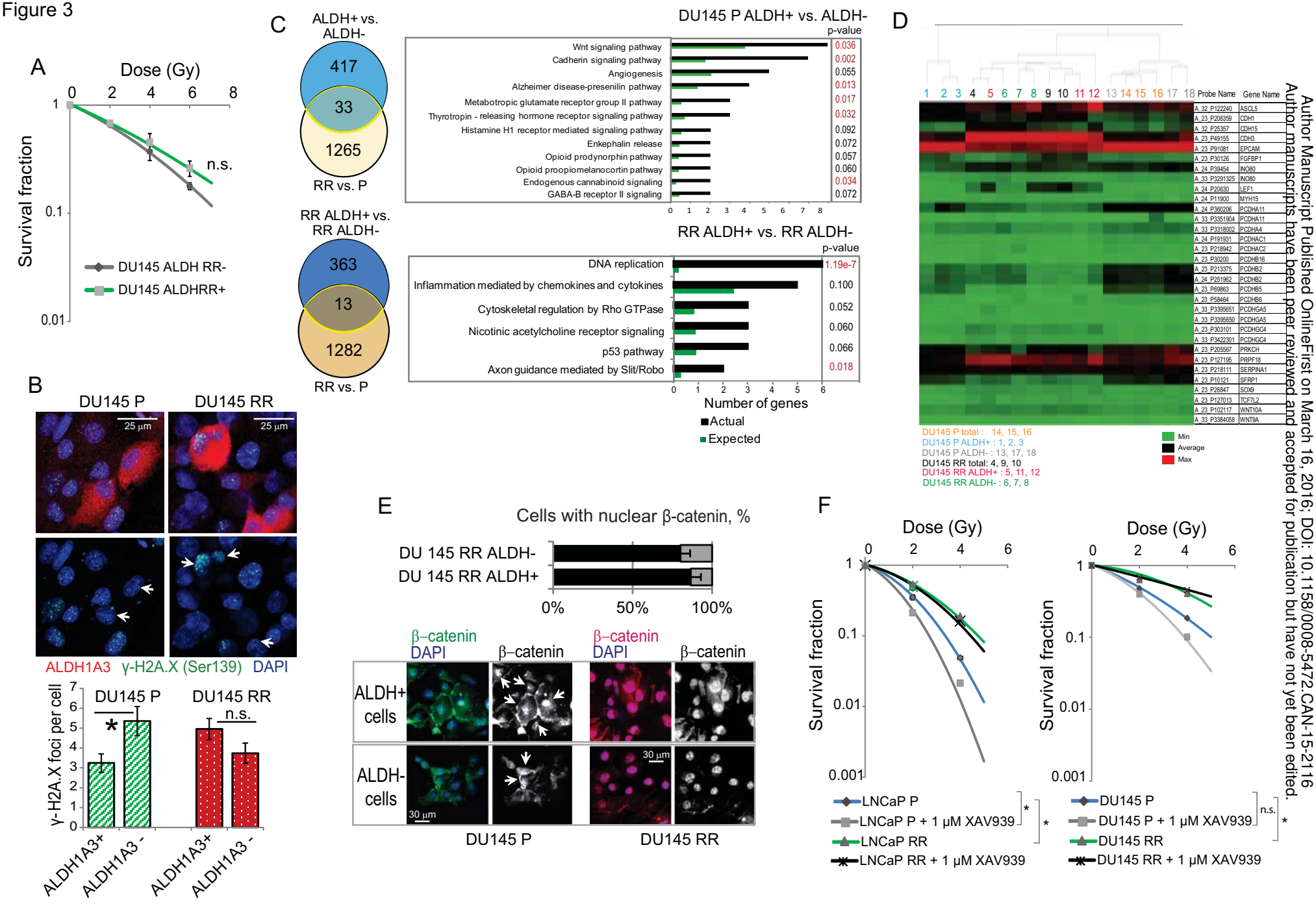

Figure 4

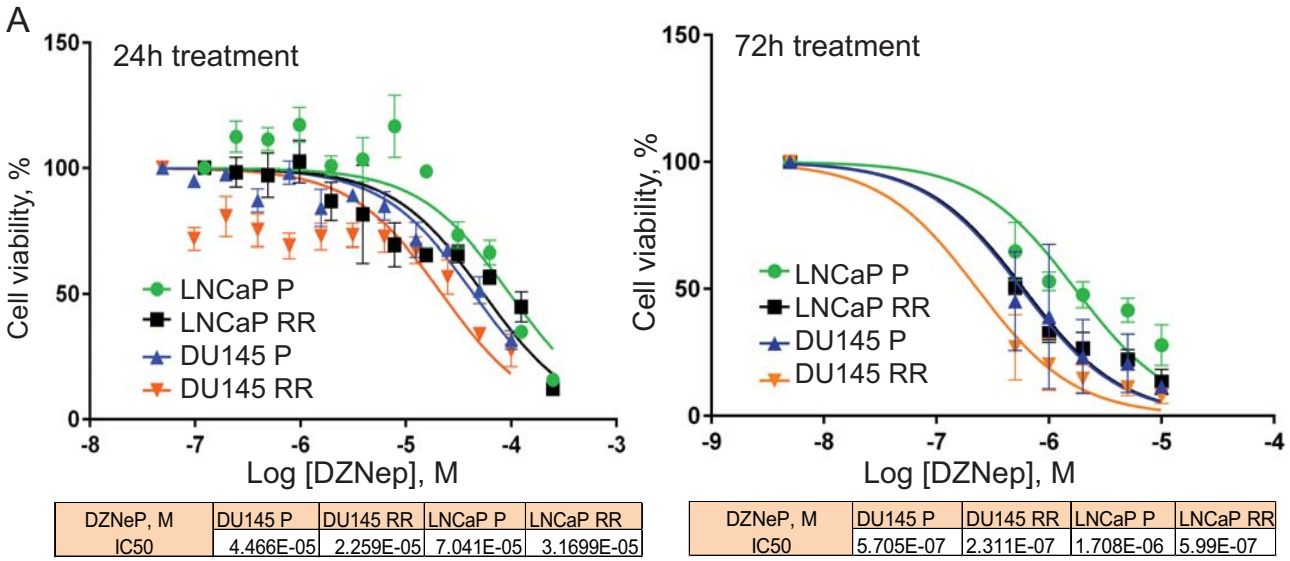


| DZNeP, M | DU145 P | DU145 RR | LNCaP P | LNCaP RR |
|---|---|---|---|---|
| IC50 | 4.466E-05 | 2.259E-05 | 7.041E-05 | 3.1699E-05 |

| DZNeP, M | DU145 P | DU145 RR | LNCaP P | LNCaP RR |
|---|---|---|---|---|
| IC50 | 5.705E-07 | 2.311E-07 | 1.708E-06 | 5.99E-07 |

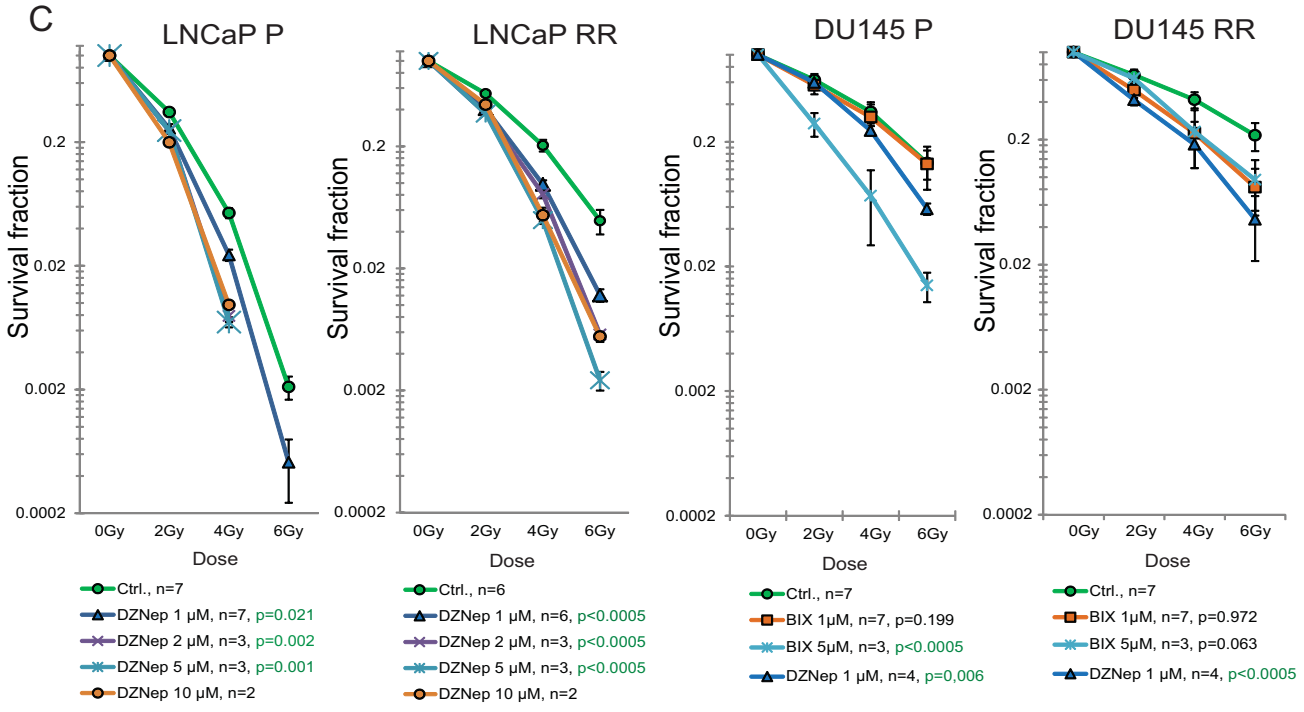


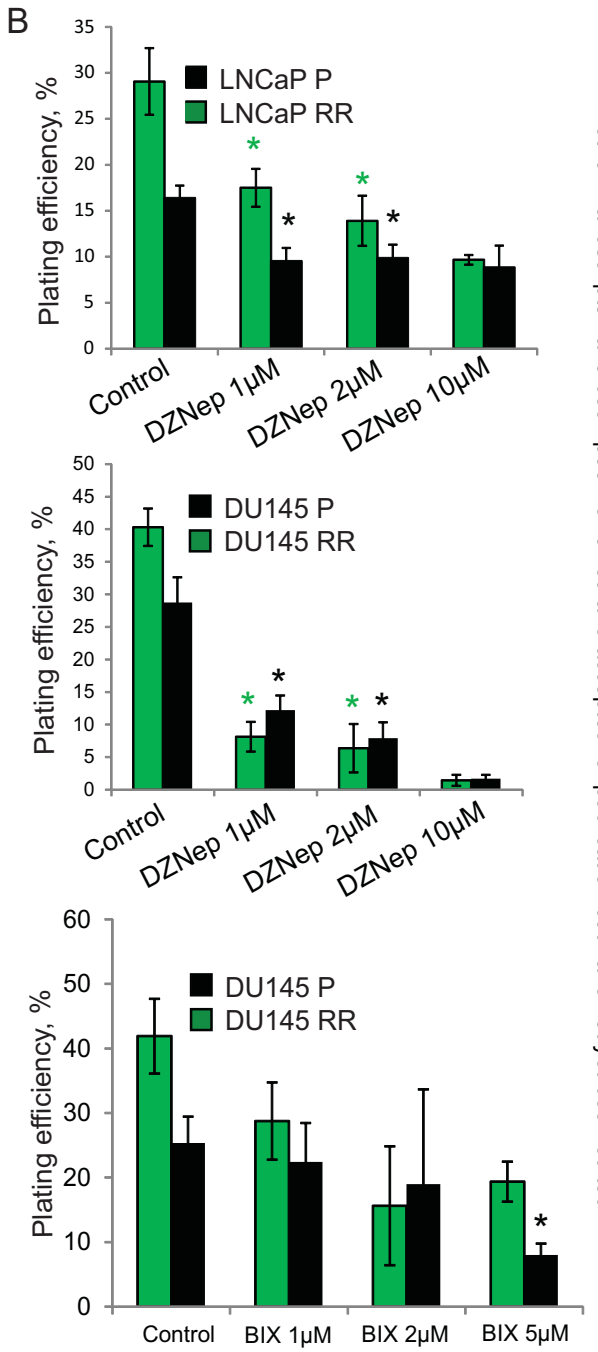

Figure 5

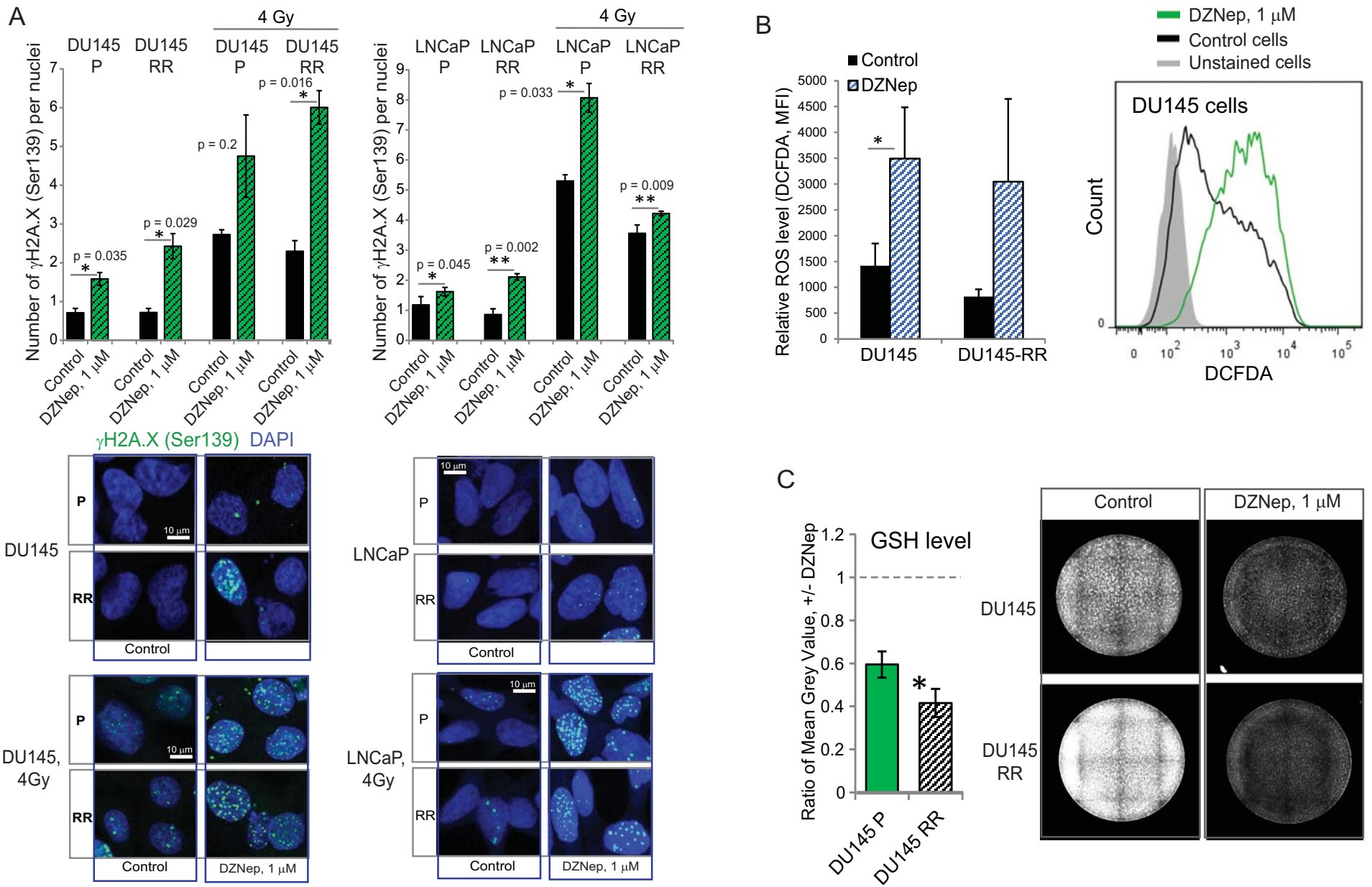

Figure 6

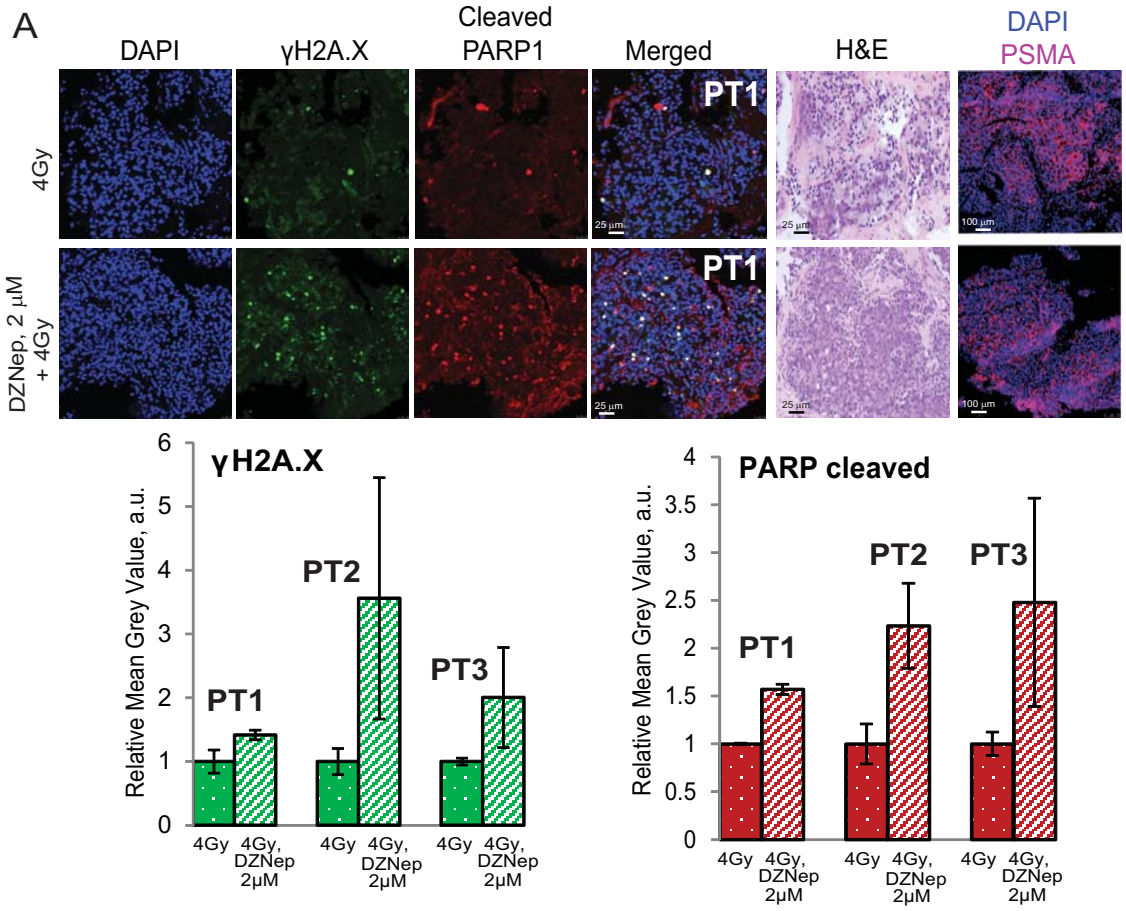


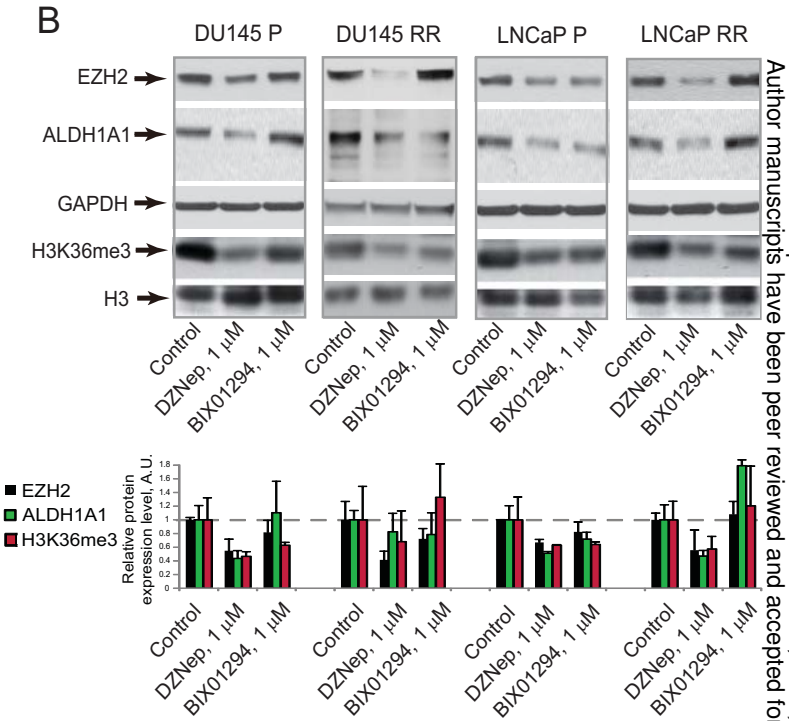


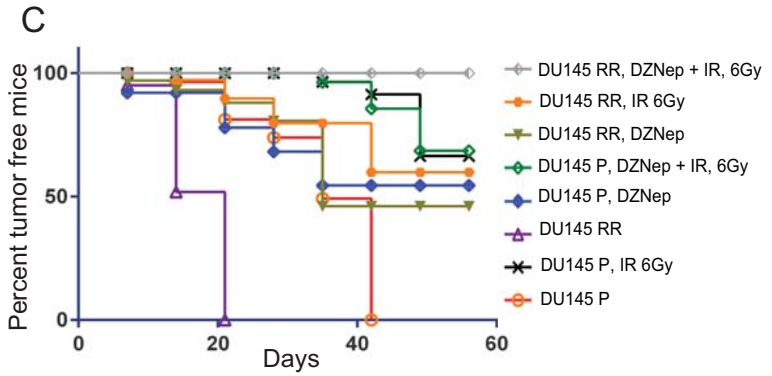


| | p-value |
|---|---|
| DU145 P vs. DU145 RR | < 0.0001 |
| DU145 P vs. DU145 P, DZNep | < 0.0001 |
| DU145 P vs. DU145 P, IR 6Gy | < 0.0001 |
| DU145 P vs. DU145 P, DZNep + IR 6Gy | < 0.0001 |
| DU145 RR vs. DU145 RR , DZNep | < 0.0001 |
| DU145 RR vs. DU145 RR, IR 6Gy | < 0.0001 |
| DU145 RR vs. DU145 RR , DZNep + IR 6Gy | < 0.0001 |
| DU145 P, IR 6Gy vs. DU145 RR, IR 6Gy | < 0.0001 |
| DU145 P, DZNep + IR 6Gy vs.DU145 RR, DZNep + IR 6Gy | 0.008 |
| DU145 P, IR 6Gy vs. DU145 RR, IR 6Gy | 0.037 |

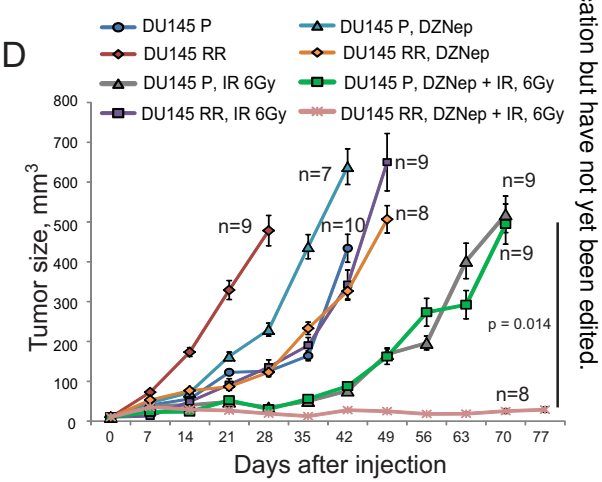

Figure 7

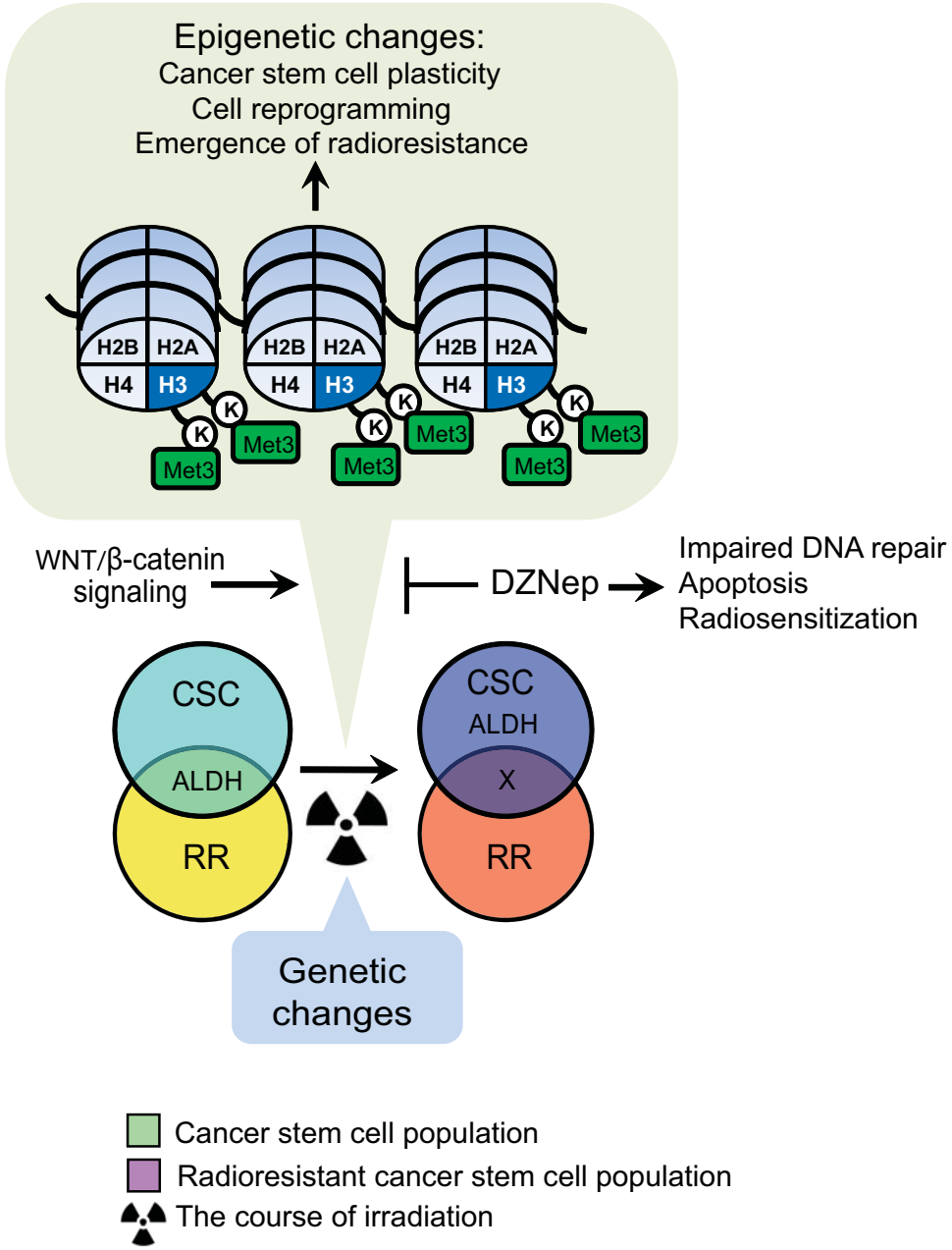

AACR American Association for Cancer Research

Cancer Research

The Journal of Cancer Research (1916–1930) | The American Journal of Cancer (1931–1940)

# An epigenetic reprogramming strategy to re-sensitize radioresistant prostate cancer cells.

Claudia Peitzsch, Monica Cojoc, Linda Hein, et al.

*Cancer Res* Published OnlineFirst March 16, 2016.